Channel and inter-channel morphology resulting from the long-term interplay of alongslope and downslope processes, NE Rockall Trough, NE Atlantic

Aggeliki Georgiopoulou[1,2]*, Michael Owens[2], Peter D.W. Haughton[2]

[1] School of Environment and Technology, University of Brighton, Cockcroft Building, Lewes Road, BN2 4GJ, UK

[2] UCD School of Earth Sciences, University College Dublin, Science Centre West, Belfield, Dublin Ireland

* Corresponding author: A.Georgiopoulou@brighton.ac.uk

Abstract

With this contribution we use a pair of overlapping 3D seismic surveys and two exploration wells to document the response of long-lived slope channels to the onset of bottom currents sweeping the lower slope in the NE Rockall Basin, offshore Ireland. Downslope gravity current activity, linked to a phase of uplift, prevailed throughout the Eocene and led to the formation of multiple channels, most notably a large-scale sinuous channel complex (Channel 4 Complex) tied to a persistent sediment entry point on the margin. Channels fed lobes on the floor of the basin, with increased axial tilting forcing gravity currents to flow parallel to the base of slope. A phase of margin-wide differential subsidence and basin deepening in the Late Eocene then activated bottom current circulation across the basin. Northward-flowing bottom currents first erosionally refashioned the lower slope creating a prominent unconformity with contourites that then initially forming infill drifts. Bottom currents swept along and obliquely upslope, building plastered drifts that straddled the lower sections of the still active channels. The drifts modified and amplified the spurs separating the active channels, with interaction between along and downslope processes accreting sediment that built and maintained channel relief and allowed the channel mouths to extend further basinward over and across the earlier lobes. Contourite-forced channel extension on account of lower slope depositional re-profiling represents another manifestation of the interplay between slope channels and bottom currents. In the case of NE Rockall, the accreted base of slope wedge and mounded geometry resembles similar features elsewhere along the eastern Rockall margin. Those have previously been ascribed to mass-transport and base-up channel initiation, however, the similarities are so striking that we propose that these also are the result of lower slope re-profiling by bottom currents.

Keywords: contourites; turbidites; channels, canyons, sediment thieving, 3D seismic, mixed systems, Antarctic Bottom Water

1. Introduction

Gravity currents are a major driver of downslope siliciclastic sediment transport in submarine environments. These episodic currents help to shape the morphology of margins by eroding and depositing sediment across the shelf-slope-basin floor profile. Sediment transported by gravity currents down a slope can either partially or wholly bypass the slope (e.g. through channels) but can also be deposited and stored on the slope. Increasingly however, the influence of semi-permanent alongslope currents is becoming recognised for the important role it plays in shaping the morphology of the slope and base of slope (e.g. Sansom, 2018). In general, alongslope or bottom currents erode the substrate and/or deposit contourites of varying scales and geometries both on slopes and in areas near the base of slope (Rebesco et al., 2014). However, they are also known to have other effects on slope systems which include steering of turbidity currents (Fonnesu et al 2020; Shanmugam et al., 1993a), reworking of gravity current sediments (Mutti and Carminatti, 2011), slope undercutting (Georgiopoulou et al., 2013) forced channel migration and the cutting of terraces leading to stepped slopes at depths where the alongslope currents are active (Zhu et al., 2010). This interaction leads to complicated deposit geometries that are not always easy to interpret. Simplistic interpretations assigning deposits to one or the other process can have significant implications in several fields, such as hydrocarbon exploration, where predicting lithological facies distributions is of paramount importance in terms of reservoir quality and seal capacity (e.g. Amy, 2019), in assessing the strength and stability of a slope and the associated geohazard (e.g. Gatter et al., 2020; Brackenridge et al., 2020; Georgiopoulou et al., 2019), and in palaeogeographic reconstructions where deposits like these are used to infer opening of oceanic gateways and new water mass connections leading to large-scale climatic changes (e.g. Jakobsson et al., 2007; Koenitz et al., 2008). As such, research in the field of bottom currents and contourites and the manner in which they interact with slopes and downslope processes (gravity currents) has been steadily increasing in the last decade. This study examines the Cenozoic evolution of the NE Rockall Trough slope offshore NW Ireland, where a series of large-scale mounded features with a complex internal architecture occur within the Eocene to Pliocene stratigraphy. The Erris Wedge, a buried wedge with variable thickness and similar stratigraphic position has been mapped to the south of the study area and has been attributed to slope instability and mass movement (Elliott et al., 2006). The aims of our study are to understand the origin of these enigmatic mounds, assess the relative contributions of alongslope and downslope processes in producing this morphology and to constrain the palaeo-bottom current circulation in this area, which was important for the connection of the water masses to the NE Atlantic.

1.1 Regional Setting

1.1.1 Physiographic Setting and Oceanography

The Rockall Trough is a NE-SW orientated, sediment-starved elongate topographic low, located west of mainland Ireland (Fig. 1). Water depths in the trough range from 1000m in the north, where it is bounded by the Wyville-Thompson Ridge, to 4000m in the south, where it opens into the Porcupine Abyssal Plain (Fig. 1). The trough is bordered to the east by the Irish Shelf and to the west by the Rockall Bank (Fig. 1). The eastern bounding slope of the trough consistently ranges in width from 30km to 40km and is incised by channels which extend from the mid-slope and the shelf edge to the base of slope (Fig. 1). South-east of the Hebrides Terrace Seamount the slope and base of slope are occupied by thick sediments associated with the Donegal-Barra Fan, a glacial trough mouth fan that drained the British Irish Ice Sheet (Armishaw et al., 2000) (Fig. 1).

Deep water circulation in the Rockall Trough started in the Late Eocene, around the same time as the opening of other oceanic gateways (the Drake Passage and the Tasmania-Antarctic Passage), that affected and collectively established the global thermohaline circulation (Zachos et al., 2001). The complex morphology of troughs, seamounts and ridges in the Rockall Trough exert a substantial control on the movement and mixing of water masses in the area. The modern circulation follows a cyclonic pattern, flowing northwards along the eastern margin, but, on encountering the rising slopes of the Wyville-Thomson Ridge, it is deflected and steered to flow southwards along the western margin (New and Smythe-Wright, 2001). Bottom current related deposits, contourite drifts and sediment waves, are common, almost everywhere in the Rockall Trough (Faugères et al., 1981; Georgiopoulou et al., 2013; Sacchetti et al., 2011; Sacchetti et al., 2012) and their distribution suggests this pattern of circulation has persisted at least since the Pliocene (Stoker, 1997).

1.1.2 Geological Setting

The Rockall Trough is underlain by the sediment-underfilled Rockall Basin which rests upon hyperextended crust (Shannon, 1991). It is one of a series of deep-water sedimentary basins along the NE Atlantic continental margin that developed in response to the Permo-Triassic break-up of Pangaea (Doré et al., 1999; Naylor and Shannon, 2005; Tyrrell et al., 2010). Seafloor spreading in the Central Atlantic began in Early-Mid Jurassic. The Late Jurassic was marked by a marine transgression and the deposition of the first marine facies (Doré et al., 1999; Tyrrell et al., 2010). Seafloor spreading propagated northwards during the Cretaceous from the SW to the NE, with thick marine strata overlying the earlier Jurassic rift (Shannon and Naylor, 2010). The Cretaceous was also marked by volcanism, which may have been critical in the formation of the basin (Scrutton and Bentley, 1988).

The post rift tectonic history of the NE Atlantic margin was characterised by three periodic, kilometre-scale vertical movements in the early, mid and late Cenozoic (Praeg et al., 2005a). A late Palaeocene-early Eocene phase of tilting occurred along the NW European margin that resulted in basinward progradation of clastic sediment from the uplifted inner continental margins as well as offshore highs (Praeg et al., 2005a). In the late Eocene – early Oligocene a phase of subsidence (sagging) occurred in which basin margins steepened due to up to 2km of differential subsidence (Praeg et al., 2005a). Subsidence rate outstripped sedimentation rate at this time causing many of the basins along the margin, particularly the Rockall Trough (due to its relative distance from source areas), to be starved of sediment (Shannon and Naylor, 1998). As a result, there was no shelf progradation during that time and sedimentation patterns along the margin were mostly characterised by deep water contourites which formed due to the onset of bottom currents (Praeg et al., 2005a; Stoker, 1998; Stoker et al., 2001b). In Rockall Basin differential subsidence and the onset of bottom current circulation caused the development of the C30 regional unconformity, an angular unconformity associated with a high amplitude reflector (Stoker et al., 2001b: their figures 5 and 6). It is suggested that slope rotation, associated with differential subsidence, resulted in widespread slope failure causing the formation of what is interpreted as a large base-of-slope mass transport deposit termed the Erris Wedge, which overlies the C30 regional unconformity and extends from the North Porcupine Bank to the southern limit of the Donegal-Barra Fan (Elliott et al., 2006). Another episode of tilting began around the Early Pliocene (Praeg et al., 2005a) which caused renewed progradation of shelf-slope clinoforms both from the uplifted inner margin as well as offshore structural highs (Praeg et al., 2005a). Oceanographic circulation also changed around this time resulting in the development of a second angular unconformity, the C10 regional unconformity (Stoker et al., 2001b).

The Neogene and Pleistocene glaciations gave rise to the Donegal Barra Fan, that sits on the C10 unconformity. This was the major focus of glacial sediment delivery, fed by ice streams that crossed the continental shelf and drained western Scotland and northwest Ireland (Bradwell et al., 2008).

2. Materials and Methods

2.1 3D Seismic data analysis

Two high resolution 3D Airgun seismic surveys, Shell 2006 and PGS-SRT 1998, were provided by Serica Energy and formed the primary data-source used to complete this study (Fig. 1). The total area covered by the overlapping 3D seismic data amounts to ca. 3000 km². Both seismic cubes are zero-phase, time migrated, 3D reflection surveys and have a normal polarity (European). The dominant frequency of the stratigraphic interval of interest (Base Eocene-Present) is approximately 40Hz. The dominant frequency along with the average velocity (1737 m s^{-1}) was used to calculate the vertical resolution, which is estimated to be ca. 11m for this interval. The PGS-SRT 1998 seismic cube has an inline (N-S) and crossline (E-W) spacing of 12.5m while the Shell 2006 seismic cube has an inline (NE-SW) and crossline (NW-SE) spacing of 25m.

Both 3D seismic cubes were pre-loaded and integrated into the Kingdom project by Serica Energy prior to being received. A mistie analysis was completed in order to ensure the datasets had been tied together correctly. This was completed in the 'Interactive Mistie analysis' feature within Kingdom. Time-shifts, phase rotations and amplitude scaling were applied to achieve accurate correlation.

Horizon mapping across the two 3D seismic surveys was carried out for key stratigraphic surfaces, which were subsequently used to generate isochron maps to examine thickness variations of stratigraphic units. Attribute analysis was also performed generating a) maps of sweetness, an empirical measure designed to highlight "sweet" spots in seismic data, which is particularly useful in areas of high acoustic impedance, b) dip of maximum similarity, a measure of similarity among a number of adjacent seismic traces, useful in highlighting discontinuities such as faults and fractures (comparable to coherency and semblance analysis), and

c) maximum amplitude attribute, that scans for highest amplitude within specified time windows and is useful in highlighting sand bodies.

2.2 Well data

Exploration wells 5/22-1 and 12/2-1 that are located in the area covered by the PGS-SRT 1998 seismic volume (Fig. 1) were used to characterize the stratigraphy and to constrain the ages of key horizons. Formation tops were also preloaded by Serica Energy into the Kingdom project. Well reports and composite logs were provided by the Petroleum Affairs Division (Supplementary Material 1).

Well 5/22-1 was an exploration well targeting Early and Late Palaeocene turbidite sandstones. Logging While Drilling (LWD) gamma ray was acquired for the upper section of the well down to 2527 m below the seafloor (mbsf) (Fig. 2). This type of gamma ray logging is a useful proxy for lithological interpretations. According to the well report, a small gap exists from 3350 – 3400 mbsf when tool exchange happened. Only conventional cuttings between 2537 – 3465 mbsf, and some sidewall cores from 3400 mbsf to the bottom of the hole at 3465 mbsf were brought to surface.

Well 12/2-1 targeted pre-rift Permo-Triassic and Jurassic sandstones in the Dooish Prospect (Fig. 3). No gamma ray or conventional cuttings were collected from the upper part of the drill site. LWD gamma ray data and cuttings exist from 2240 mbsf onwards. In comparison to well 5/22-1 this well had poor data quality for the Cenozoic section and so it was not used in calibrating the seismic and in the time-depth conversion.

2.3 Time-depth conversion

Ideally time-depth conversions require velocity data, but this was not available for this project, so the "no velocity data" method was used. In this method a relationship between interpreted seismic horizons and formation tops is established creating in this way pairs of two-way time to well depth. The software then creates a velocity model for the conversion from the time domain to the depth domain. The more pairs entered the more accurate the conversion. For this study 6 pairs were created at well 5/22-1. Time-depth conversion was only performed at the well location and not to the entire seismic volume as there are a lot of complex structures and the velocity model would have been unreliable away from the well location.

3. Results

Three seismic units were identified, units A, B and C. These are bound by three prominent seismic horizons the ages of which have been determined by well biostratigraphy (Figs 2 and 3) and by correlation with published work (Magee et al., 2014); these are the Base Eocene Reflector (BER), and the C30 and the C10 unconformities.

3.1 Seismic stratigraphy

3.1.1 Base Eocene Reflector (BER)

The BER is a prominent, continuous, moderate-to-high amplitude reflector, correlated and mapped throughout both seismic volumes. It is conformable with the underlying Palaeocene strata and gradually dips to the west and northwest, albeit more steeply in the southern part of the study area compared to the north. It is characterised by two zones of very high-amplitude discontinuous reflections (Channels 2 and 3) (Fig. 4). The southern zone is 200 m wide, largely linear, with a sinuosity of 1.14 and extends across the full width of the seismic data (Channel 4) (Fig. 4). To the west the zone (Channel 4) widens to a lobate patch (Fig. 4). A second channel, approximately 12 km to the south, has similar width and exhibits sinuosity of 1.17, but it is shorter and not visible up-dip (Channel 5) (Fig. 4).

The BER is locally offset by small-scale faults that have a polygonal geometry in plan-view (Figs 3 and 4). The sweetness, dip of maximum similarity, and the coherency attribute volumes pick out the widespread development of polygonal faulting. The polygonal faults do not affect the areas proximal to or within the channels (Fig. 4a).

3.1.2 C30 Unconformity (Late Eocene)

The C30 unconformity is a distinct high-amplitude reflector which is continuous throughout the area. Amplitude variations on this surface reveal a series of erosional and depositional features. Four channels are identified on this surface, numbered 2 to 5 (Fig. 5).

The channels along the C30 unconformity are E-W to SE-NW orientated in the northern part of the study area (Fig. 5). In seismic section, their bases appear to truncate the reflectors of the underlying Unit A stratigraphy (Fig. 6c). In the south of the study area, a large-scale SE-NW orientated, sinuous (sinuosity = 1.44) channel, with a width 1.6-3.1 km is identified (Channel 4). The base of this channel is broad and characterised by high amplitudes (Figs 5 and 6). To the south, another less sinuous channel (Channel 5), 2km wide, with elongate low- and high-amplitude stripes, parallel to the channel axis and an orientation NE-SW is also identified (Figs 5 and 6).

Faulting on the C30 unconformity comprises what appears to be both tightly-spaced polygonal normal faulting on the slope and well-developed polygonal faulting near the base of slope (Fig. 5b). In plan view, the normal faulting pattern on the slope is either concave-downslope or concave-upslope, creating lense-shaped geometries (Figs 5b and c). The faults affect the stratigraphy above and below the C30 unconformity. At the base of slope, the plan view pattern of the faulting is more typically polygonal (Fig. 5b). The faulting is not present in the vicinity or inside the southernmost channel (Fig. 5c).

3.1.3 C10 Unconformity (Pleistocene)

The C10 unconformity is a high-amplitude reflector that is locally offset by small-scale faults, but not to the same degree as the previous reflectors or the stratigraphy underneath (Fig. 3). It is continuous throughout the extent of the study area, mapped on the shelf edge in the north, on the slope and near the base of slope in the south and southwest. It truncates the underlying stratigraphy of Unit B, forming an angular unconformity. The erosional effects of C10 are more evident in the south of the study area and along the shelf edge in the north (Fig. 3).

3.2 Seismic facies

3.2.1 Unit A

Unit A is bounded at the base by the BER and at the top by the C30 unconformity. It is characterised by discontinuous low-to-moderate reflections and in places by high amplitude reflections contained within channels (Fig. 3). It is difficult to map individual reflectors for any distance within this unit and it appears highly disrupted, almost chaotic (Fig. 3).

Sweetness and dip of maximum similarity attribute maps sliced through Unit A reveal the presence of at least five channels numbered 1-5 from north to south (Figs 4 and 7). Channels 2, 3, 4 and 5 can also be seen on the BER surface but do not incise below it (Fig. 3b). Channel 1 is not seen on the BER suggesting that it did not incise down to that stratigraphic level. All the channels are roughly orientated E-W near the lower part of the unit, but, through time, they appear to change orientation, with the exception of channel 3 that retains the same orientation (Figs 4 and 7).

Channel 1 disappears in the shallower sections of the unit, while channel 2 swings to a NE-SW orientation. Channels 2 and 3 are relatively narrow, no more than 400m wide, and largely straight in the lower parts of the unit. Channel 3 disappears half-way through the unit, but Channel 2 persists and becomes wider, reaching 5-7 km width (Fig. 4c). Some smaller channels developed in the middle of the unit that may be tributaries to Channel 2, but they are not long-lived.

The Channel 4 margins are well defined in all the time slices and appear to define a broad, but confined feeder, approximately 4km wide. In cross-section, Channel 4 appears to contain smaller channel elements that aggrade and locally show evidence of migration (Fig. 7), making it a channel complex, and thus from now on referred to as the Channel 4 Complex. The channel complex is flanked by low amplitude seismic packages. It is meandering with increasing sinuosity (from 1.11 to 1.51) through time (Fig. 7). Throughout the lower part of Unit A it opens to the west to wider lobate features at all stratigraphic levels, which in cross section appear mounded and therefore depositional (Fig. 4d). The position of these lobate features also swings as the orientation of the channel changes (Fig. 4). The seismic character of the lobate features is of moderate-to-high amplitude semi-parallel reflections and are separated by low-amplitude sequences. In the upper levels of the lower part of Unit A (Figs 7a-c), the Channel 4 Complex is composed of feeder channels that occupy the areas that lower in the stratigraphy were between the channel margins and the low-amplitude packages. Their orientation maintains that of the Channel 4 Complex but in the upper parts of unit A, they develop a nearly 90^{o} bend at the base of slope and become oriented NNE-SSW, parallel to the slope (Fig. 7c).

Channel 5 maintains the same width of nearly 4 km and the same orientation through the lower part of Unit A (Figs 4a-c) but becomes wider in the shallower parts. Internal reflections are not as high amplitude as for the Channel 4 Complex, and although Channel 5 also appears to contain smaller channel elements, these are not as clearly defined. The channel margins are marked by a change to areas characterized by low-amplitude seismic reflections (Figs 4a-c) that in cross-section appear constructional and mounded (Fig. 4d). In the upper part of Unit A, Channel 5 disappears.

Between Channel 3 and the Channel 4 Complex there is an area of striped high-amplitude patches orientated NW-SE (Figs 4b and c). These are visible in the lower 100ms of Unit A but disappear over time. In cross section they appear flat, with no evidence of channelisation, erosion or deposition (Fig. 4d).

3.2.2 Unit B

Unit B is of Late Eocene to Plio-Pleistocene age and broadly corresponds with the regional RTc and RTb megasequences of Stoker et al. (2001). The base of Unit B is the C30 unconformity and it is bound at the top by the C10 (Pleistocene) unconformity (Fig. 3). The RTc and RTb megasequences of Stoker et al. (2001a) are separated by the C20 unconformity. However, in the study area the C20 reflector (or reflective zone) is not expressed. According to Stoker et al. (2001a) the C20 reflector (or reflective zone) onlaps the C30 reflector near the basin margins. Due to its absence from the study area we infer that this onlap is outside of the 3D seismic volume.

Unit B is divided in two subunits, B1 and B2 (Figs 3 and 8). The sub-units are separated by a semi continuous, moderate to high-amplitude reflector (Fig. 8) that is not easily traceable throughout the study area. The sub-units are thus distinguished primarily based on their differing seismic facies rather than by a distinct reflector. The reflector that separates them is not necessarily equivalent to C20, so we are not equating sub-units B1 and B2 to RTb and RTc. The age of this reflector cannot be determined due to gaps in the cuttings collected at this level in the well. It is inferred to be of Pliocene age based on its stratigraphic position in relation to the limited cuttings data (Fig. 2). In well 5/22-1, Unit B has a thickness of 800m (Fig. 2).

3.2.2.1 Sub-unit B1

Sub-unit B1 is characterised by moderate amplitude reflections in the lower half, and moderate-to-low amplitude in the upper half (Fig. 2). Sub-unit B1 reflections are predominantly discontinuous but can be occasionally continuous (for up to several kilometres). It should be noted that pervasive faulting in the sub-unit does also add to the discontinuous nature of reflections, although this does not appear to be the main cause of reflection discontinuity. High-amplitude, discontinuous and chaotic reflections continue to occur in erosional, U-shaped features in the South of the study area.

Sub-unit B1 has been further subdivided into B1 Lower and B1 Upper (Fig. 6). B1 Lower and B1 Upper do not form part of the seismic stratigraphic framework as they do not have margin-wide significance but rather they represent two different styles of deposition which are locally important.

B1 Lower is characterised by low to moderate amplitude, continuous, although heavily faulted, reflections (Fig. 3). Its upper surface (Top of B1 Lower - Fig. 6) is smooth and sub-horizontal which contrasts with the topographically variable nature of the C30 unconformity. Seismic reflectors also show onlap relationships with C30 and the thickness map of the sub-unit in general mirrors the topography of C30 and thickness maxima are located within the channels that run across C30 (Fig. 8). It is evident that this unit healed the topography of C30 below (Fig. 8c). However, in the south of the study area, Channel 5 that truncates Unit A, persists and is also present on the ‘Top of B1 Lower’ surface (Fig. 9a). The Channel 4 Complex also persists through to sub-unit B2.

Two thick (up to 500ms) mounded sedimentary features comprise B1 Upper, the Northern Mound (NM) and Southern Mound (SM) (Figs 9 and 10, respectively). They are characterised predominantly by low to moderate-amplitude (occasionally high-amplitude) reflections (Figs 9 and 10). The reflections are generally continuous, although heavily faulted, and wavy in nature (Figs 9 and 10). They were deposited unconformably on top of the B1 Lower sequence, on the slope and the base of slope. The mounds thin upslope showing a wedge-shaped geometry and have an orientation along and oblique to slope (Figs 9 and 10). Thinning appears to be controlled by erosion as evidenced by the truncations against the C10 unconformity (Figs 8c and 9b).

The Northern Mound can be divided in two stacked parts, NM1 and NM2. NM1 sits unconformably on the Top B1 Lower reflector and has an approximate thickness of 300m at well 5/22-1. NM2 sits on top of NM1, has an erosional base and approximate thickness of 200m at well 5/22-1. The base of NM2 is coeval with the development of a slope parallel to oblique (NE-SW orientated) channel (moat) which incises in NM1 (Fig. 9).

The southern reaches of SM deposited at the base of slope and on the inter-channel ridges associated with Channel 5. Here the morphology and thickness of the mounds are more subdued, but by contrast to the northern area, display greater overall complexity in terms of geometry. To the north of Channel 5 smaller elongate mounds developed in a N-S orientation, with inter-mound channels forming in the same orientation between them, whereas to the south of the channel, a series of similar size equant mounds developed in no specific orientation and with larger inter-mound areas (Fig. 10). The elongate mounds north of the channel are internally characterized by sub-horizontal high and low amplitude reflections, transitioning to wavy reflections further upslope forming large-scale waveforms which build upslope onto the inter-channel ridge of Channel 5 (Fig. 10). The equant mounds south of the channel are internally characterized by low-to-moderate amplitude reflections inclined towards the slope (Fig. 10). Internal reflections within the mounds adjacent to Channel 5 appear truncated.

These mounds are also faulted but the faults are not as closely spaced as in the NM and SM mounds.

3.2.2.2 Sub-unit B2

A significant change in seismic facies occurs in sub-unit B2 when compared with sub-unit B1. B2 comprises predominantly low to moderate amplitude wavy reflections which are continuous in nature (Figs 8 and 9). In some areas these wavy reflections form what appear to be large-scale waveforms (Fig. 10c) which build upslope on top of the sub-unit B1 reflectors. Reflections appear to be less affected by faulting in this seismic sub-unit when compared with sub-unit B1.

In the Shell 2006 dataset, moderate amplitude, semi-continuous, less chaotic reflections occur in the channels at this stratigraphic level (Fig. 10b). This contrasts with the high amplitude, discontinuous and chaotic reflections in the directly underlying units A and B1 (Figs 10b and c).

Longitudinal bedforms of high seismic amplitude are found within an alongslope channel and within a perpendicular to slope channel (Channel 2) (Fig. 10d). This surface is most notable for a series of incisional features, some of which were initiated at this time while others persist from the Eocene (Figs 10c and d). In places, the base of sub-unit 2 appears to truncate reflectors of sub-unit B1 (Fig. 10d).

In the south of the study area, Channel 5 persists at this level and has a south-easterly orientation in its lower part and rotates to an E-W orientation in its upper part (Fig. 10d). The basal surface of the channel truncates the reflectors of sub-unit B1 forming steep channel walls to the north and south. The steep walls of the channel are onlapped by low-to-moderate amplitude, continuous, and discontinuous reflections of the channel fill (Fig. 10). Near the upper parts of the channel infill, the reflections continue across to the inter-channel ridge and merge with mound-shaped deposits (Fig. 10c).

The Channel 4 Complex also persists into sub-unit B2 as a sinuous erosional channel that exceeds 3km in width (Fig. 10c). In seismic section, the channel walls are shallower dipping than they were within sub-unit B1, however, it still erodes into sub-unit B1 reflectors (Fig. 10c).

Throughout the study area, the top of sub-unit B2 is truncated by the overlying C10 regional unconformity which often results in partial erosion of sub-unit B2 but in some places completely removes it (Fig. 10b). Truncation of sub-unit B2 reflectors appears to be most prevalent on topographic highs (Fig. 10c).

Sub-unit B2 is the thickest in the north where it forms a NE-SW orientated mound, within the axis of Channel 5, on the adjacent inter-channel ridge to the north where it forms a large mound and in the westernmost corner of the dataset (Figs 10c and d). Smaller mounds can also be found in this southern area, mostly accreting in the inter-channel ridges. Their internal reflectors however are not restricted to these ridges, instead they appear to connect with the upper part of the Channel 5 fill (Figs 10c and d). In cross section, parallel to the slope, the small mounds are in fact waveforms that build upslope and are very similar to the waveforms in sub-unit B1. The waveforms appear truncated by the C10 unconformity further upslope (Fig. 10c).

The elongate mound in the north is internally characterized by horizontal to sub-horizontal low-to-moderate amplitude continuous reflections that are mildly wavy (Fig. 9b). In an upslope direction, the mound is thinned by erosion along the C10 unconformity.

Polygonal faulting in sub-unit B2, where present, appears to only affect the sequence near the base.

3.2.3 Unit C

Unit C differs markedly from the units below in terms of its acoustic characteristics. It is characterised by stacked packages of chaotic internal character with low-to-moderate amplitudes (Figs 3, 6, 9, 10). They are separated by high-amplitude, sub-horizontal to steeply-dipping reflectors that are generally continuous for tens of kilometres but are abruptly truncated by overlying or adjacent packages (Figs 3, 6, 9, 10). Unit C is described and discussed in detail by Roy et al. (2020).

3.3 Well Stratigraphy

Constraints on the lithology and stratigraphy are based on well reports (Supplementary Material 1). The Palaeocene-Eocene boundary (Base Eocene = base of seismic unit A) is found at 3400 m, marked by a lithological change from calcareous claystone with silty, glauconitic sandy and tuffaceous horizons below to a substantial decrease of tuffs and a decrease in gamma response above (Fig. 2). The C30 unconformity (Late Eocene) was identified at 2738 m in well 5/22-1 based on a marked decrease in gamma-ray (Fig. 2), sonic travel time and neutron porosity and a sharp increase in formation density and resistivity (Supplementary Material 1). The base of the Pleistocene, the C10 unconformity, is recognised by a relatively sharp change in gamma ray response at 1937 m (Fig. 2).

According to the well report sandstones and siltstones are rare near the Paleocene-Eocene boundary but become more common up hole, within our unit A (Supplementary Material 1). The claystones become increasingly less tuffaceous above 3250 m, and from 3250m to 3093m claystone is the dominant lithology but there are occasional siltstones, sandstones (<10%) and rare thin stringers of micritic limestone (Fig. 2). From 3093m to 2738m siltstones (<30%) and sandstones (<10%) are present near the base but their abundance decreases up hole.

There is an increase in carbonate content above the C30 unconformity at 2738m. Overall, the gamma-ray response in the interval 2738m to 2537m (sub-unit B1 Lower) averages 60 API indicating it is likely shale-dominated but does contain siltier and sandier intervals (Fig. 2). However, the gamma-ray caliper log spiked on multiple occasions indicating the presence of artificial variations in gamma ray response throughout parts of this sequence (Fig. 2).

Throughout the interval between 2738m to 2537m claystone is described as containing inter-beds (1-2m thick) of quartzose sandstone with variable grain size from very fine to fine-grained with moderate rounding and sorting (Supplementary Material 1). From 2537m to 2380m the gamma ray was logged through twenty-inch casing muting the gamma ray response (Fig. 2). From 2380m to 1937m (sub-units Upper B1 and B2) a low gamma-ray response (15 API) is maintained and despite the absence of a caliper log a constant response indicates it may be reliable for this part of the well (Fig. 2). The low gamma-ray response (15 API) from 2537m to 1937m thus probably reflects an increase in silty or sandy lithologies (Fig. 2). Occasional spikes in the gamma ray response, for example at 2045m and 2270m, may be the result of inter-bedding with shales in an otherwise silty or sand prone sequence, although this is uncertain given the absence of caliper log (Fig. 2).

LWD gamma-ray above the C10 unconformity shows that the API ranges from 30 API at the base of the sequence to 45 in the upper part of the sequence (up to 1720m) indicating that this unit (which corresponds to our unit C) is likely a silty or shale-prone sequence overall but becoming more shaley upwards (Fig. 2).

4. Discussion

4.1 Slope-evolution

Unit A is dominated by channels of various scales indicating that large-scale slope incision initiated at the start of the Eocene (Fig. 4). The channels' presence had varying durations. Some persisted through to the overlying units while others died out, with this likely reflecting the persistence of certain sediment point sources and the shorter-term activation and abandonment of others.

The largest and longest-lived system is the Channel 4 Complex. It was active between the early Eocene and the end of the Miocene suggesting a long-lived point source on the margin (Fig. 6c). A mature channel with extensive up-dip erosion incising the shelf edge can be seen on the present-day seafloor towards the southern end of the study area (Fig. 1) indicating a persistent morphological control that promoted repeated re-occupation of channels on this sector of the slope with an orientation that tended to swing quite freely. The low-amplitude deposits that border its margins are interpreted as levees, due to their seismic character of low to moderate amplitude and continuous reflections, their wedge-shaped geometry (Figs 6c, 8, 11) and the silty lithology (Unit A). At the downslope termination of the complex, lobate constructional mounds are tied to changes of channel orientation (Fig. 4c). The element stacking seen in this complex is characterized by net deposition at the start, evidenced by lobe deposits, and later progradation of the system (Fig 4 vs Fig. 7). The channel terminal lobes show clear evidence of compensational stacking (Fig. 4d), with the channel switching position most likely when the lobe deposits reach threshold thicknesses that the active flows could no longer overcome and as a result were re-directed towards topographically low points (Straub et al., 2009).

Channel 5 that is located south of the Channel 4 Complex, appears to have also been long-lived and it too has a present-day equivalent channel in the same location (Fig. 1). It was responsible for substantial erosion of Unit A as seen by the truncation of reflectors (Fig. 6c). It contains smaller channels and must have been a significant agent of sediment transfer from the slope to the basin (Fig. 11). It also opened out to form depositional lobes, but it is more difficult to document the temporal changes in this system as it is at the southern edge of the data (Figs 7 and 11).

The extensive downslope gravity driven slope incision seen in this stratigraphic interval (Unit A) is probably a response to the reported tilting that took place in the Palaeocene-Eocene and resulted in basinward progradation of shelf-slope wedges from uplifted blocks along the inner continental margin and from offshore highs (Praeg et al., 2005b). Examples of this in the stratigraphic record can be found in the northern Porcupine and southern Rockall basins (McDonnell and Shannon, 2001) and in other areas along the margin. Although gravity currents may have initiated at the sites of the channels in the early Eocene (lower parts of Unit A), the main phase of channel incision appears to have been during the middle Eocene. Lithologies on the slope are dominated by silty claystone with very little sand present, while deposits within the channel show that they acted as conduits for higher efficiency flows by-passing the slope and potentially depositing sand to the SW and beyond the area covered by the 3D seismic data.

Moreover, during the Middle Eocene gravity current activity persisted at the site of the Channel 4 Complex forming a leveed sinuous channel complex and feeder channels, suggesting that upslope source areas that developed during the early Cenozoic phase of tilting (Praeg et al., 2005b) continued to supply sediment to the system at this time. At the base of slope, the Channel 4 Complex is interpreted to link up with a series of slope-parallel channels which first appear at this time (Fig. 7). The inferred slope-parallel flow suggests the presence of a significant axial topographic gradient. This gradient is inferred to have been caused by the formation of the Hebrides Terrace Seamount, a volcanic centre located immediately to the NW of the study area (Fig. 1). Pulsing of the Iceland Plume in the early Eocene is thought to be the source of this volcanic centre as well as a number of other volcanic centres within the Rockall Trough (Ritchie et al., 1999a). The wider pattern of Middle Eocene uplift and subsidence (Praeg et al., 2005b) may also have been a factor that helped to develop an axial trough gradient.

According to Praeg et al. (2005a), mid-Cenozoic sagging (differential subsidence) of late Eocene to early Oligocene age was widespread along the NE Atlantic margin and resulted in the termination of shelf wedge progradation. Bottom currents, as a result of differential subsidence and basin deepening, initiated at this time and contourite deposition began to occur along the margin. In the Rockall Basin, this phase of differential subsidence is recorded by the development of the C30 regional unconformity (Stoker et al., 2001a) which is present throughout the study area.

The effects of mid Cenozoic differential subsidence are recorded in the stratigraphic record within the study area. Thus, C30 is associated with re-excavation of the Middle Eocene Channel 5, possibly in response to slope rotation which may also have been responsible for the rejuvenation of the Channel 4 Complex or the excavation of a new channel at the same site.

Despite evidence for continuing downslope transport (Channel 5), a new style of depositional process becomes dominant after the late Eocene (post-C30, Unit B) in the area (Fig. 11). Early deposition appears to heal the variability seen in the C30 surface topography as evidenced by the smoothing and infilling of channels (Fig. 8c) and the onlap relationship observed between the reflectors of subunit B1 Lower and the C30 unconformity (Fig. 9). This is followed by the buildup of large-scale mounds (NM and SM) and a change in lithology which becomes siltier and sandier. Based on the mound geometry (mounded and elongate oblique to slope), their internal acoustic character (low-to-moderate amplitude, wavy continuous reflectors), upslope accretion and lithological characteristics (increased silt and sand content) they are interpreted as elongate, partially plastered contourite drifts (Rebesco et al., 2014) (Figs 8-11). In certain areas, these accumulations formed large-scale waveforms that modified the slope and base of slope topography (B1 Upper and B2) (Fig. 10). Important contourite deposition continued into the Miocene (sub-unit B2; Fig. 10). Concurrently with contourite deposition, channels continued to act as conduits for gravity currents, with a more fixed orientation than in pre-C30, and with coarser lithologies as suggested by the higher amplitudes and the lack of polygonal faulting. Polygonal faulting tends to occur in fine grained lithologies (Antonellini and Mollema, 2015; Cartwright et al., 2003; Watterson et al., 2000). The polygonal faults appear to terminate in areas proximal to the channel bodies (Fig. 5) demonstrating the coarser nature of the channels.

Both the timing and mechanism of channel formation suggested here contrast markedly with previous interpretations, most notably with Elliott et al. (2006) who attributed channel formation to widespread slope failure associated with a phase of rapid late Eocene (C30) differential subsidence that excavated the channels. This may be the case in other areas along the eastern margin of the Rockall Trough. However, in the case of the Channel 4 Complex, it is apparent that at least some of the channels along the eastern margin of the trough initiated prior to the development of the C30 surface (late Eocene).

Late Cenozoic tilting of Plio-Pleistocene age promoted basinward progradation of shelf-slope sediment wedges from the inner margins and from offshore highs along the NE Atlantic margin once again (Praeg et al., 2005b). This coincides with the development of the C10 regional unconformity of Stoker et al. (2001a) within the study area, throughout the Rockall Trough and further afield along the margin. In the study area, basinward tilting is reflected in the stratigraphic record by progradation of a series of mass transport deposits (MTDs) (Figs 2, 3, 6, 10) associated with the development of the Donegal-Barra Fan. The MTDs locally utilised older Middle Eocene and Late Eocene channels (see above) as conduits but gradually backfilled them, eventually muting the relief (Fig. 10). The Pleistocene MTD succession is not the focus of this paper, but is analysed in detail in Roy et al. (2020).

4.2 Phases of mound development

The evidence we have examined suggests that the mounds are the complex product of interacting downslope and alongslope processes. We recognize them as long-lived constructional features that originally developed from an erosional seascape, perhaps as old as Middle Eocene and prior to the development of the C30 unconformity (Late Eocene) that marks the onset of bottom current circulation in the area. Several phases of contourite deposition, from the Late Eocene and ending by the Pleistocene, resulted in amplification of the erosional seascape to form the mounds. Below we propose a sequence of their depositional history.

Phase 1- Mound initiation and generation of relief (Mid to Late Eocene)

Processes at this time were dominated by downslope gravity currents culminating in the development of leveed channel complexes (Channels 2 and 5, and the Channel 4 Complex (Fig. 12a). Channel formation generated corrugations on the slope, with the generation of this relief representing an important stage in the development of the mounds subsequently (Fig. 12a), particularly with regards to Channel 5. The channel itself acted as a conduit for gravity currents. However, the adjacent inter-channel ridge associated with Channel 5 was a positive relief feature built by pelagic drape sediments and levee deposits overspilling from both the Channel 4 Complex and Channel 5 (Fig. 12b). The first appearance of slope-parallel channels which link to the Channel 4 Complex, show evidence for the early development of alongslope transport by gravity currents (Fig. 12b). It is important to note that these north-to-south flowing features initiated prior to the onset of bottom current activity (pre-C30) crucially suggesting that evidence for alongslope transport is not necessarily an indication of bottom current activity.

Phase 2- Bottom current modification of earlier relief (Late Eocene- Mio/Pliocene)

A marked change in the style of sedimentation occurred in the Late Eocene in association with differential subsidence, the onset of strong bottom current circulation and the development of the C30 unconformity. This change is recorded in the initiation of alongslope bottom-current processes and contourite deposition. In terms of the mounds, this change represents an important phase in their history as downslope gravity currents began to interact with alongslope bottom currents. In association with the development of the C30 regional unconformity, Channel 5 was re-excavated creating a shallower conduit compared to the Middle Eocene channel, particularly further downslope (Fig. 12c). Moreover, a smaller secondary channel initiated at the site of the Channel 4 Complex (or itself was renewed) (Fig. 12c) which generated further relief between the channels (Fig. 12c). Downslope gravity currents were active within these conduits. Coupled with this, bottom currents began to deposit contourites across the slope, amplifying the inter-channel ridge topography (Fig. 12c). Palaeo-bottom current orientations at the time were orientated approximately NNE-SSW (Fig. 12c – green arrows), parallel to a large contourite moat in the north of the area (Fig. 9). The source of these bottom currents is thought to be from the south as previously suggested by Stoker et al. (2001a), as there is no evidence to suggest northerly-derived bottom currents.

Phase 3- Continued mound amplification (Mio/Pliocene- Pleistocene)

Coupled channel and inter-channel ridge deposition persisted during the Miocene (sub-unit B2) (Fig. 12d). Both Channel 5 and the Channel 4 Complex continued to act as conduits for gravity currents (Fig. 12d). However, bottom current activity came to dominate the depositional regime. The dominance of bottom current activity is highlighted by the presence of low-amplitude continuous reflections throughout the inter-channel ridge deposits and the channel infill (Fig. 10). Moreover, contourites are plastered onto the walls of Channel 5 (Fig. 10b) further highlighting bottom current activity within the channel. Correlation of channel reflectors with those on the inter-channel ridge at this time (Fig. 10) suggests that channel and inter-channel ridge bottom current deposition were linked, particularly nearer the base of slope (Fig. 11). As a result, Channel 5 is interpreted to have been actively sequestering contouritic sediment at this time in addition to bottom currents draping the ridge (Fig. 12d). The source of this sediment is thought to have been derived either externally and subsequently swept into the channel or to have reworked the deposits of gravity currents around the channel. However, it is apparent that sediment was also being swept out of the channel onto the adjacent inter-channel ridge to the north (Fig. 12). Palaeo-bottom currents continued to be orientated in a SSW-NNE trend as indicated by longitudinal bedforms located in the north of the area (Figs 10d). It is likely that preferential sequestration of contourites and trapping of sediment in Channel 5 (the most southerly channel) starved the Channel 4

Complex of sediment which reinforces the suggestion that bottom currents were southerly derived. The palaeoslope minimum water depth reach of these currents can be roughly estimated at about 2200m (the depth of the C10 unconformity, taking a sound velocity of 1.5 km s^{-1} for the water and 2km s^{-1} for the 0.3s average thickness of the Pleistocene). Sea level during the Pliocene was less than 50m higher than present day so even with that taken into account this is approximately the water depth where the Antarctic Bottom Water sweeps the eastern slope of the Rockall Trough. We tentatively suggest that AABW entered the Rockall Trough from the south, probably at the same time as general bottom current activity started in the area (C30, base of sub-unit B1) with North Atlantic Deep Water coming in from the north along the western trough margin, through the Faroe-Shetland Channel (Davies et al., 2001), but intensified and became significant during the Pliocene (upper B1 and B2). By Pleistocene times, glacial sediment delivery dominated and overprinted any bottom current activity that might have still been present.

4.3 Wider significance

Elliot et al (2006) mapped a buried base of slope wedge termed the Erris Wedge overlapping with the southern part of the study area and running southwestwards along the Rockall margin towards the Porcupine Bank for over 160 km. They characterised it using widely-spaced 2D seismic data and recognised two seismic facies; a lower more chaotic sequence and an upper one with sub-parallel continuous reflections, similar to the character of unit B. The wedge was attributed to mass transport processes related to instability triggered by Late Eocene slope rotation coinciding with the C30 unconforrmity, and the slope failures were thought to have triggered the formation of canyons by a bottom-up mechanism (Elliott et al., 2006). Although less well imaged in the 2D data, the Erris Wedge resembles the base of slope wedge described here as part of Unit B, suggesting a rather different origin. Bottom-currents moving northeastwards along the base of slope may have interacted with channels more widely along the whole length of the margin. The thickness of the Erris Wedge reveals distinctive thick patches (up to 700 m) between a number of mapped channels (Elliot et al., 2006, their figure 12) which may reflect an element of pirating or reworking of channel sediments by bottom currents. This would also suggest that the interaction of alongslope and downslope processes has influenced the lower slope architecture along other sectors of the Irish Rockall Trough margin.

A complex interplay between downslope and alongslope processes has been recognized on many continental margins. Bottom currents that impinge on slopes can interact with the channels and the gravity currents passing through them (Fig. 13a-e). This can involve the two processes operating synchronously or alternating one with the other (Fonnesu et al., 2020; Mulder et al., 2008). The bottom currents can thus strip sediment from the upper and diluted parts of the sediment gravity flows, sweeping fines into augmented down-drift levees (Fig. 13a) (Fonnesu et al., 2020; Michels et al., 2002), or in some cases building large hybrid levee drifts that accrete and force channels to migrate counter to the direction of bottom current flow (Fig. 13b) (Fonnesu et al., 2020; Sansom, 2018). In other cases, channels can capture and divert bottom currents (Fig. 13c). In the Gulf of Cadiz, the Portimao Canyon captures sediment from alongslope bottom currents and conducts it downslope preventing thick contourite drifts from developing on the lee side of the channels (Marchès et al., 2007). In the South China Sea, the intensification of alongslope bottom current circulation during the Miocene swept sediment into channels, forcing them to step laterally, in this case in the direction of bottom current flow (Fig. 13d) (Gong et al., 2013). Bottom currents operating deeper on the slope may partially rework or even detach basin floor fans emerging from feeder channels (Mutti and Carminatti, 2011).

The NE Rockall slope provides an example of yet another way in which bottom-currents and their deposits can interact with downslope processes (Fig. 13e). In this case, bottom currents swept the base of slope and the lower reaches of already well-established channels, before obliquely climbing upslope to form plastered drifts on a healed section of the mid slope further to the north. Infill and then multi-crested drifts straddled the still active channels in the south, locally contributing sediment to the channel fills but also draping the spurs between channels. Sediment was locally carried from the channels by bottom currents to the inter-channel areas helping to build and maintain channel relief. As both the Channel 4 Complex and Channel 5 were tied to persistent sediment entry points and prominent incisions on the upper slope, sediment gravity flows were able to continually re-flush and maintain the conduits. Rather than forcing the channels to migrate laterally, the bottom current deposits in this case allowed the channels to extend basinward by providing additional lateral confinement. Sustained contourite accretion thus produced a base of slope wedge nearly 1 km thick that re-profiled the lower slope and allowed the channels to extend basinwards over basin floor deposits by over 10 km. Growth of the wedge reset the equilibrium profile for the gravity currents, allowing the channel fills to aggrade as they extended further into the basin. A similar process appears to have been active on the Uruguayan margin in the Late Cretaceous, although there it does not appear as pronounced and the channels show evidence of some lateral migration (Creaser et al., 2017). However, these two examples show that this type of interaction may not be uncommon.

5. Conclusions

Channel complexes, compensationally stacked lobes, and a number of individual sinuous channel elements, demonstrate dominance of downslope transport during the Eocene, possibly in response to tilting (coeval uplift and subsidence) of the margin (Praeg et al., 2005b).

Important inter-channel relief was generated by the extended period of gravity current channelisation. We show that the timing of channel incision (mid Eocene) pre-dates slope rotation associated with the C30 unconformity (late Eocene) which is contrary to previous interpretations.

Onset of bottom current circulation in the Late Eocene, caused by differential subsidence and basin deepening, resulted in contourite deposition that at first muted the relief and continued until the Pleistocene causing amplification of the earlier erosional seascape to form large-scale inter-channel mounds.

From the Mio/Pliocene to the Pleistocene, alongslope bottom currents came to dominate, resulting in continued deposition of contourites throughout the area. During this time, bottom currents were active within the channels and actively swept sediment in and out of them, further amplifying the inter-channel ridge relief. Interestingly, channel position was not affected by the powerful effect of the bottom currents as demonstrated elsewhere where the two processes strongly interact, suggesting intense channelisation by the two forces combined kept the channels in place and prevented them from migrating.

The waterdepth on the palaeoslope where these currents operated matches that of the Antarctic Bottom Water. That would tentatively suggest the time it entered into the Rockall Trough from the south was in mid Miocene and that it intensified during the Pliocene.

Evidence for bottom currents interacting with channels can be found on margins throughout the world however, the style of interaction seen on these margins varies considerably between them. Some of the ways in which this interaction manifests include; 1) bottom current forced channel migration, South China Sea (Zhu et al., 2010), 2) bottom current deflection of channel axes, Argentinian margin (Hernández-Molina et al., 2009) 3) Sediment pirating of channel deposits, Argentinian margin (Hernández-Molina et al., 2009) 4) bottom current flow capture by channels, Gulf of Cadiz (Marchès et al., 2007), and 5) from the current study in the NE Rockall Trough, bottom current reworking of in-channel deposits and redeposition onto and amplification of the inter-channel ridge relief leading to the formation of large-scale (>1 km high) mounded features.

Acknowledgements

The authors wish to thank Serica Energy for funding for MO's MRes and access to data. We are also grateful to the Department of the Environment, Climate and Communications of the Irish Government and the formerly known as the Petroleum Affairs Division for access to data. Graham Prichard and Clara Altobell are acknowledged for entrusting us with the project. We are grateful to Dr Marco Fonnesu and one anonymous reviewer for their constructive reviews which helped improve the manuscript significantly.

Data availability

We are not authorized to share the data that was made available to us by Serica Energy and the Department of the Environment, Climate and Communications (DECC) of the Irish Government for the purposes of this study. However, all data used in this study can be viewed and directly requested through the DECC website (https://www.gov.ie/en/service/search-petroleum-exploration-and-production-data/).

References

Amy, L.A., 2019. A review of producing fields inferred to have upslope stratigraphically trapped turbidite reservoirs: Trapping styles (pure and combined), pinch-out formation, and depositional setting. AAPG Bulletin 103, 2861-2889.

Antonellini, M., Mollema, P.N., 2015. Polygonal deformation bands. Journal of Structural Geology 81, 45-58.

Armishaw, J.E., Holmes, R.W., Stow, D.A.V., 2000. The Barra Fan: A bottom-current reworked, glacially-fed submarine fan system. Marine and Petroleum Geology 17, 219-238.

Brackenridge, R.E., Nicholson, U., Sapiie, B., Stow, D., Tappin, D.R., 2020. Indonesian Throughflow as a preconditioning mechanism for submarine landslides in the Makassar Strait. Geological Society, London, Special Publications 500, 195-217.

Bradwell, T., Stoker, M.S., Golledge, N.R., Wilson, C.K., Merritt, J.W., Long, D., Everest, J.D., Hestvik, O.B., Stevenson, A.G., Hubbard, A.L., Finlayson, A.G., Mathers, H.E., 2008. The northern sector of the last British Ice Sheet: Maximum extent and demise. Earth-Science Reviews 88, 207-226.

Cartwright, J., James, D., Bolton, A., 2003. The genesis of polygonal fault systems: a review. Geological Society, London, Special Publications 216, 223-243.

Creaser, A., Hernández-Molina, F.J. , Badalini, G., Thompson, P., Walker, R., Soto, M., Conti, B., 2017. A Late Cretaceous mixed (turbidite-contourite) system along the Uruguayan Margin: Sedimentary and palaeoceanographic implications. Marine Geology 390, 234-253.

Davies, R., Cartwright, J., Pike, J., Line, C., 2001. Early Oligocene initiation of North Atlantic Deep Water formation. Nature 410, 917-920.

Doré, A.G., Lundin, E.R., Jensen, L.N., Birkenland, Ø., Eliassen, P.E., Fichler, C., 1999. Principal tectonic events in the evolution of the northwest European Atlantic margin. Geological Society, London, Petroleum Geology Conference, series 5, 41-61.

Elliott, G.M., Shannon, P.M., Haughton, P.D.W., Praeg, D., O'Reilly, B., 2006. Mid- to Late Cenozoic canyon development on the eastern margin of the Rockall Trough, offshore Ireland. Marine Geology 229, 113-132.

Faugères, J.C., Gonthier, E., Grousset, F., Poutiers, J., 1981. The Feni Drift: The importance and meaning of slump deposits on the Eastern slope of the Rockall Bank. Marine Geology 40, M49-M57.

Fonnesu, M., Palermo, D., Galbiati, M., Marchesini, M., Bonamini, E., Bendias, D., 2020. A new world-class deep-water play-type, deposited by the syndepositional interaction of turbidity flows and bottom currents: The giant Eocene Coral Field in northern Mozambique. Marine and Petroleum Geology 111, 179-201.

Fuhrmann, A., Kane, I.A., Clare, M.A., Ferguson, R.A., Schomacker, E., Bonamini, E., Contreras, F.A., 2020. Hybrid turbidite-drift channel complexes: An integrated multiscale model. Geology 48, 562-568.

Gatter, R., Clare, M.A., Hunt, J.E., Watts, M., Madhusudhan, B.N., Talling, P.J., Huhn, K., 2020. A multi-disciplinary investigation of the AFEN Slide: the relationship between contourites and submarine landslides. Geological Society, London, Special Publications 500, 173-193.

Georgiopoulou, A., Krastel, S., Finch, N., Zehn, K., McCarron, S., Huvenne, V.A.I., Haughton, P.D.W., Shannon, P.M., 2019. On the Timing and Nature of the Multiple Phases of Slope Instability on Eastern Rockall Bank, Northeast Atlantic. Geochemistry, Geophysics, Geosystems 20, 594-613.

Georgiopoulou, A., Shannon, P.M., Sacchetti, F., Haughton, P.D.W., Benetti, S., 2013. Basement-controlled multiple slope collapses, Rockall Bank Slide Complex, NE Atlantic. Marine Geology 336, 198-214.

Gong, C., Wang, Y., Zhu, W., Li, W., Xu, Q., 2013. Upper Miocene to Quaternary unidirectionally migrating deep-water channels in the Pearl River Mouth Basin, northern South China Sea. AAPG Bulletin 97, 285-308.

Hernández-Molina, F.J., Paterlini, M., Violante, R., Marshall, P., de Isasi, M., Somoza, L., Rebesco, M., 2009. Contourite depositional system on the Argentine Slope: an exceptional record of the influence of Antarctic water masses. Geology 37, 507-510.

Howe, J.A., Harland, R., Hine, N.M., Austin, W.E.N., 1998. Late Quaternary stratigraphy and palaeoceanographic change in the northern Rockall Trough, North Atlantic Ocean. Geological Society, London, Special Publications 129, 269-286.

Jakobsson, M., Backman, J., Rudels, B., Nycander, J., Frank, M., Mayer, L., Jokat, W., Sangiorgi, F., O'Regan, M., Brinkhuis, H., King, J., Moran, K., 2007. The early Miocene onset of a ventilated circulation regime in the Arctic Ocean. Nature 447, 986-990.

Koenitz, D., White, N., McCave, I.N., Hobbs, R., 2008. Internal structure of a contourite drift generated by the Antarctic Circumpolar Current. Geochemistry, Geophysics, Geosystems 9.

Magee, C., Jackson, C.A.-L., Schofield, N., 2014. Diachronous sub-volcanic intrusion along deep-water margins: insights from the Irish Rockall Basin. Basin Research 26, 85-105.

Marchès, E., Mulder, T., Cremer, M., Bonnel, C., Hanquiez, V., Gonthier, E., Lecroart, P., 2007. Contourite drift construction influenced by capture of Mediterranean Outflow Water deep-sea current by the Portimão submarine canyon (Gulf of Cadiz, South Portugal). Marine Geology 242, 247-260.

McCartney, M.S., Mauritzen, C., 2001. On the origin of the warm inflow to the Nordic Seas. Progress in Oceanography 51, 125-214.

McDonnell, A., Shannon, P.M., 2001. Comparative Tertiary stratigraphic evolution of the Porcupine and Rockall basins. Geological Society, London, Special Publications 188, 323-344.

Michels, K.H., Kuhn, G., Hillenbrand, C.D., Diekmann, B., FÜtterer, D.K., Grobe, H., Uenzelmann-Neben, G., 2002. The southern Weddell Sea: combined contourite-turbidite sedimentation at the southeastern margin of the Weddell Gyre. Geological Society, London, Memoirs 22, 305.

Mulder, T., Faugères, J.C., Gonthier, E., 2008. Chapter 21 Mixed Turbidite–Contourite Systems, in: Rebesco, M., Camerlenghi, A. (Eds.), Developments in Sedimentology. Elsevier, pp. 435-456.

Mutti, E., Carminatti, M., 2011. Deep-water sands of the Brazilian offshore basins, AAPG International Conference and Exhibition, Milan, Italy pp. 1-42.

Naylor, D., Shannon, P.M., 2005. The structural framework of the Irish Atlantic Margin. Geological Society, London, Petroleum Geology Conference, series 6, 1009-1021.

New, A.L., Smythe-Wright, D., 2001. Aspects of the circulation in the Rockall Trough. Continental Shelf Research 21, 777-810.

O'Connor, J.M., Stoffers, P., Wijbrans, J.R., Shannon, P.M., Morrissey, T., 2000. Evidence from episodic seamount volcanism for pulsing of the Iceland plume in the past 70 Myr. Nature 408, 954.

Praeg, D., Stoker, M.S., Shannon, P.M., Ceramicola, S., Hjelstuen, B., Laberg, J.S., Mathiesen, A., 2005a. Episodic Cenozoic tectonism and the development of the NW European 'passive' continental margin. Marine and Petroleum Geology 22, 1007-1030.

Praeg, D., Stoker, M.S., Shannon, P.M., Ceramicola, S., Hjelstuen, B., Laberg, J.S., Mathiesen, A., 2005b. Episodic Cenozoic tectonism and the development of the NW European ‘passive’ continental margin. Marine and Petroleum Geology 22, 1007-1030.

Rebesco, M., Javier Hernández-Molina, F., Van Rooij, D., Wåhlin, A., 2014. Contourites and associated sediments controlled by deep-water circulation processes: State-of-the-art and future Considerations. Marine Geology, 111-154.

Ritchie, J.D., Gatliff, R.W., Richards, P.C., 1999a. Early Tertiary magmatism in the offshore NW UK margin and surrounds. Geological Society, London, Petroleum Geology Conference series 5, 573-584.

Ritchie, J.D., Gatliff, R.W., Richards, P.C., 1999b. Early Tertiary magmatism in the offshore NW UK margin and surrounds. Geological Society, London, Petroleum Geology Conference series 5, 573-584.

Roy, S., Georgiopoulou, A, Benetti, S., Sacchetti, F., 2020. Mass transport deposits in the Donegal Barra Fan and their association with British_Irish Ice Sheet dynamics. Geological Society, London, Special Publications 500, 567–586.

Sacchetti, F., Benetti, S., Georgiopoulou, A., Dunlop, P., Quinn, R., 2011. Geomorphology of the Irish Rockall Trough, North Atlantic Ocean, mapped from multibeam bathymetric and backscatter data. Journal of Maps 2011, 60-81.

Sacchetti, F., Benetti, S., Georgiopoulou, A., Shannon, P.M., O'Reilly, B.M., Dunlop, P., Quinn, R., Ó Cofaigh, C., 2012. Deep-water geomorphology of the glaciated Irish margin from high-resolution marine geophysical data. Marine Geology 291-294, 113-131.

Sansom, P., 2018. Hybrid turbidite-contourite systems of the Tanzanian margin. Petroleum Geoscience 24, 258–276.

Scrutton, R.A., Bentley, P.A.D., 1988. Major Cretaceous volcanic province in southern Rockall Trough. Earth and Planetary Science Letters 91, 198-204.

Shanmugam, G., Spalding, T., Rofheart, D., 1993a. Process sedimentology and reservoir quality of deep-marine bottom-current reworked sands (sandy contourites): an example from the Gulf of Mexico. AAPG Bulletin 77, 1241-1259.

Shanmugam, G., Spalding, T.D., Rofheart, D.H., 1993b. Traction structures in deep-marine, bottom-current-reworked sands in the Pliocene and Pleistocene, Gulf of Mexico. Geology 21, 929-932.

Shannon, P.M., 1991. The development of Irish offshore sedimentary basins. Journal of the Geological Society 148, 181-189.

Shannon, P.M., Naylor, D., 1998. An assessment of Irish offshore basins and petroleum plays. Journal of Petroleum Geology 21, 125-152.

Shannon, P.M., Naylor, D., 2010. Petroleum Geology of Ireland. Dunedin Academic Press.

Stoker, M., Van Weering, T.C., Svaerdborg, T., 2001a. A mid-to late Cenozoic tectonostratigraphic framework for the Rockall Trough. Geological Society, London, Special Publications 188, 411-438.

Stoker, M.S., 1997. Mid- to late Cenozoic sedimentation on the continental margin off NW Britain. Journal of the Geological Society 154, 509-515.

Stoker, M.S., 1998. Sediment-drift development on the continental margin off NW Britain, in: Stoker, M.S., Evans, D., Cramp, A. (Eds.), Geological processes on continental margins: sedimentation, mass-wasting and stability. Geological Society Special Publication, London, pp. 229-254.

Stoker, M.S., van Weering, T.C.E., Svaerdborg, T., 2001b. A Mid- to Late Cenozoic tectonostratigraphic framework for the Rockall Trough, in: Shannon, P.M., Haughton, P.D.W., Corcoran, D.V. (Eds.), The petroleum exploration of Ireland's offshore basins. Geological Society Special Publication, London, pp. 411-438.

Straub, K.M., Paola, C., Mohrig, D., Wolinsky, M.A., George, T., 2009. Compensational stacking of channelized sedimentary deposits. Journal of Sedimentary Research 79, 673-688.

Tyrrell, S., Souders, A.K., Haughton, P.D.W., Daly, J.S., Shannon, P.M., 2010. Sedimentology, sandstone provenance and palaeodrainage on the eastern Rockall Basin margin: evidence from the Pb isotopic composition of detrital K-feldspar. Geological Society, London, Petroleum Geology Conference, series 7, 937-952.

Watterson, J., Walsh, J., Nicol, A., Nell, P., Bretan, P., 2000. Geometry and origin of a polygonal fault system. Journal of the Geological Society 157, 151-162.

Zachos, J., Pagani, M., Sloan, L., Thomas, E., Billups, K., 2001. Trends, Rhythms, and Aberrations in Global Climate 65 Ma to Present. Science 292, 686-693.

Zhu, M., Graham, S., Pang, X., McHargue, T., 2010. Characteristics of migrating submarine canyons from the middle Miocene to present: Implications for paleoceanographic circulation, northern South China Sea. Marine and Petroleum Geology 27, 307-319.

Figure captions

Figure 1. Shaded relief bathymetric map of the NE Rockall Trough showing the location of the study area with the wells and the red boxes representing the 3D seismic volumes. The major current circulation is shown with blue dashed arrows. The purple dashed lines show the extent of the Donegal Barra Fan (DBF). Also shown are the extent of the Erris Wedge in the current study area (yellow-shaded area) from Elliot et al. (2006) and the location of their figure 11. The inset shows the greater geographical location. HTS: Hebrides Terrace Seamount; WTR: Wyville Thomson Ridge; RB: Rockall Bank; ADS: Anton Dohrn Seamount; RT: Rockall Trough; PS: Porcupine Seabight; GB: Great Britain; EIRE: Ireland; FR: France.

Figure 2. Depth-converted seismic section through well 5/22-1 with well stratigraphy, gamma log, geological timescale overlain and corresponding seismic facies (Units A to C).

Figure 3. (a) Seismic section A-B illustrates the correlation of key seismic reflectors between wells 5/22-1 and 12/2-1. (b) Seismic section C-D illustrates the correlation of key surfaces across both the PGS-SRT 98' and Shell 2006 seismic cubes (indicated with red boxes on location map).

Figure 4. Sweetness attribute on (a) flattened timeslice of Base Eocene Reflector, (b) a parallel surface 0.076 s above BER and (c) a parallel surface 0.128 s above BER. (d) Seiimic profile AB as shown on (b), flattened to BER and the two timeslices of (b) and (c). The light blue surface is a mid-unit A surface with no significant stratigraphic significance but continuous enough to help with amplitude extractions within unit A (see fig. 7).

Figure 5. C30 regional unconformity with (a) sweetness attribute showing Channels 2 and 3, the Channel 4 Complex and Channel 5; (b) dip of maximum similarity and (c) zoom to the southern part showing polygonal faults preferentially developing in the inter-channel areas but largely absent within the channels.

Figure 6. (a) Surface map in TWT of the C30 regional unconformity (base of Unit B) with the most important features highlighted. Position of seismic sections AB and CD of (b) and (c) are also indicated. (b) Seismic section AB highlighting topographic lows on the C30 unconformity. (c) Seismic section CD highlighting the persistence of Channel 5 on the C30 unconformity and the incision of the Channel 4 Complex.

Figure 7. (a) Sweetness attribute on mid-unit A surface (cyan on d). (b) Sweetness on timeslice 0.068s above (a) and (c) sweetness on timeslice 0.180s above (a). The three selected timeslices show the development of slope-parallel channels and the persistence of the Channel 4 Complex and Channel 5. Note that Channel 4

Complex increases in sinuosity higher in the stratigraphy (c). Seismic section on (d) shown in (b) as CD dashed line.

Figure 8. Isochron (thickness) maps of (a) subunit B1 Lower showing the healing effect of draping over the C30 unconformity, (b) B1 Upper showing thick units forming contourite mounds NM and SM, both of which tend to thin upslope and which are separated by a contourite moat carved at the base of sub-unit B2 and (c) subunit B2 that fills the topographic lows. Seismic lines AA' and BB' are shown on figure 9.

Figure 9. (a) Seismic section AA' and (b) BB' highlighting the thickness variations of B1 Upper and B2. Positions of AA' and BB' shown on figure 8.

Figure 10. (a) Isochron map of B1 Upper contourites from the Shell 2006 dataset. Seismic sections (b) AB and (c) CD crossing the contourite drifts. The drifts are plastered to the slope with waveforms building upslope (wavy blue arrow) onto the inter-canyon ridge associated with Channel 5. (d) Sweetness attribute of the base of sub-unit B2 showing linear features parallel and perpendicular to the strike of the slope. Positions of (b) and (c) are highlighted on (a). Location of figures relative to the rest of dataset is indicated on figures 8b and 8c.

Figure 11. (a) Shaded relief bathymetric map showing the position of seismic sections (b) to (e) located within the Shell 2006 dataset. (b)-(e) A series of upslope to downslope seismic sections highlighting the variability of the Channel 5 and inter-channel ridge architecture.

Figure 12. Summary depositional evolution for the studied NE Rockall slope. (a) Early to mid-Eocene reconstruction (lower part of Unit A) emphasizing channel initiation and down-slope sediment transport. SB is shelf break; BOS the base of slope. (b) Mid to late Eocene interval (upper Unit A) highlighting south-westward deflection of gravity flow systems to run parallel to the base of slope and evolution of Channel 4 Complex. (c) Late Eocene to Mio-Pliocene with onset of bottom currents and initial accretion of drifts across the lower and mid slope (Unit B1). (d) Mio-Pliocene to Pleistocene (Unit B2) showing continued contourite accretion and wedge growth promoting canyon extension.

Figure 13. Contrasting stratigraphic outcomes of the interaction between down- and along-slope processes: (a) pirating of flow tops and heightened levee asymmetry (Michels et al. 2004; Shanmugam et al. 1993); (b) forced migration counter to bottom currents by up-current accretion of levee drifts (Sansom 2018, Fonnesu al. 2020, Fuhrmann et al., 2020); (c) capture and diversion of bottom currents by channels (Marchès et al., 2007) ; (d) lateral stepping forced by spilling of contour current sediment into channel (e.g. Gong et al. 2013), and (e)

channel downslope extension on account of accretion and base of slope re-profiling as detailed for the NE Rockall area in this paper.

Supplementary Material 1

Well IRE 5/22-1 “Errigal Deepwater Exploration” Final Well Report. Volume 1: Geological and Petrophysical Evaluation. Republic of Ireland Continental Shelf Oil Well Records. Report provided by the Petroleum Affairs Division (PAD). Available for download from: https://www.gov.ie/en/publication/63e171-oil-and-gas-exploration-production-data/

Well IRE 5/22-1 “Wellsite litholog for ERRIGAL”. Provided by the Petroleum Affairs Division (PAD). Available for download from: https://www.gov.ie/en/publication/63e171-oil-and-gas-exploration-production-data/

Well IRE 12/2-1 “Dooish composite log. Report provided by the Petroleum Affairs Division (PAD). Available for download from: https://www.gov.ie/en/publication/63e171-oil-and-gas-exploration-production-data/

Figure 1

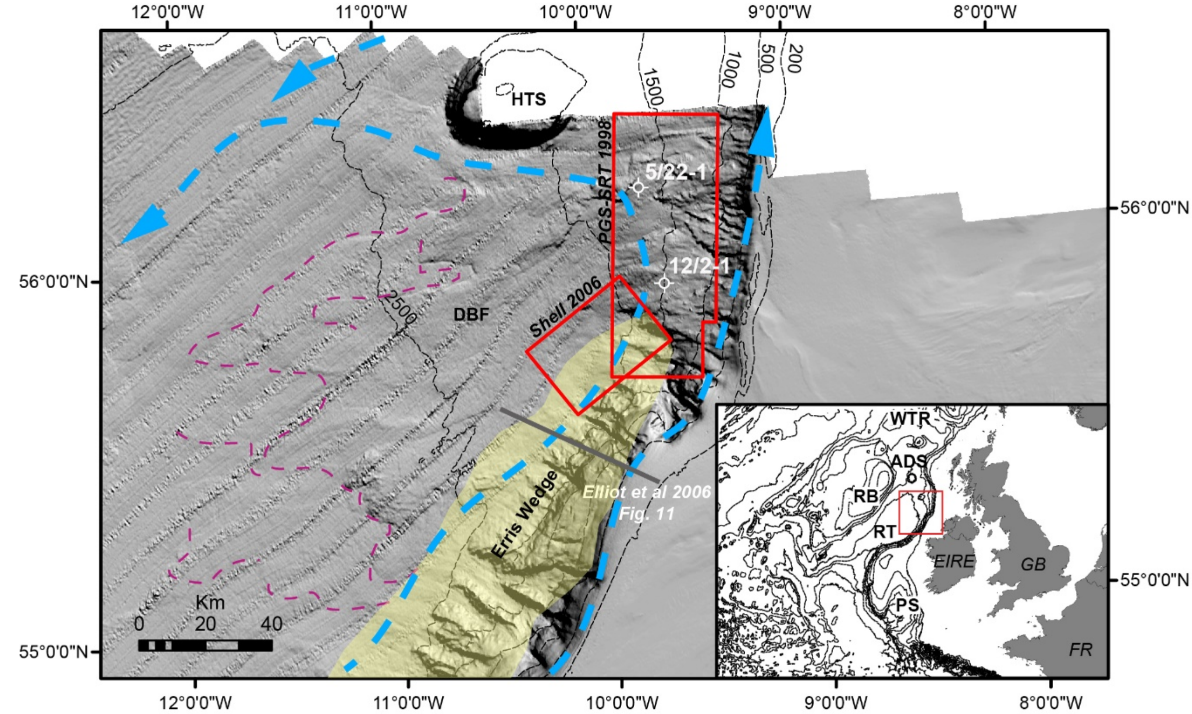

12°0'0"W
11°0'0"W
10°0'0"W
9°0'0"W
8°0'0"W
56°0'0"N
55°0'0"N
HTS
1500
1000
500
200
2500
PGS-SRT 1998
5/22-1
12/2-1
Shell 2006
DBF
Erris Wedge
Elliot et al 2006
Fig. 11
Km
0
20
40
WTR
ADS
RB
RT
EIRE
GB
PS
FR

836 Figure 2

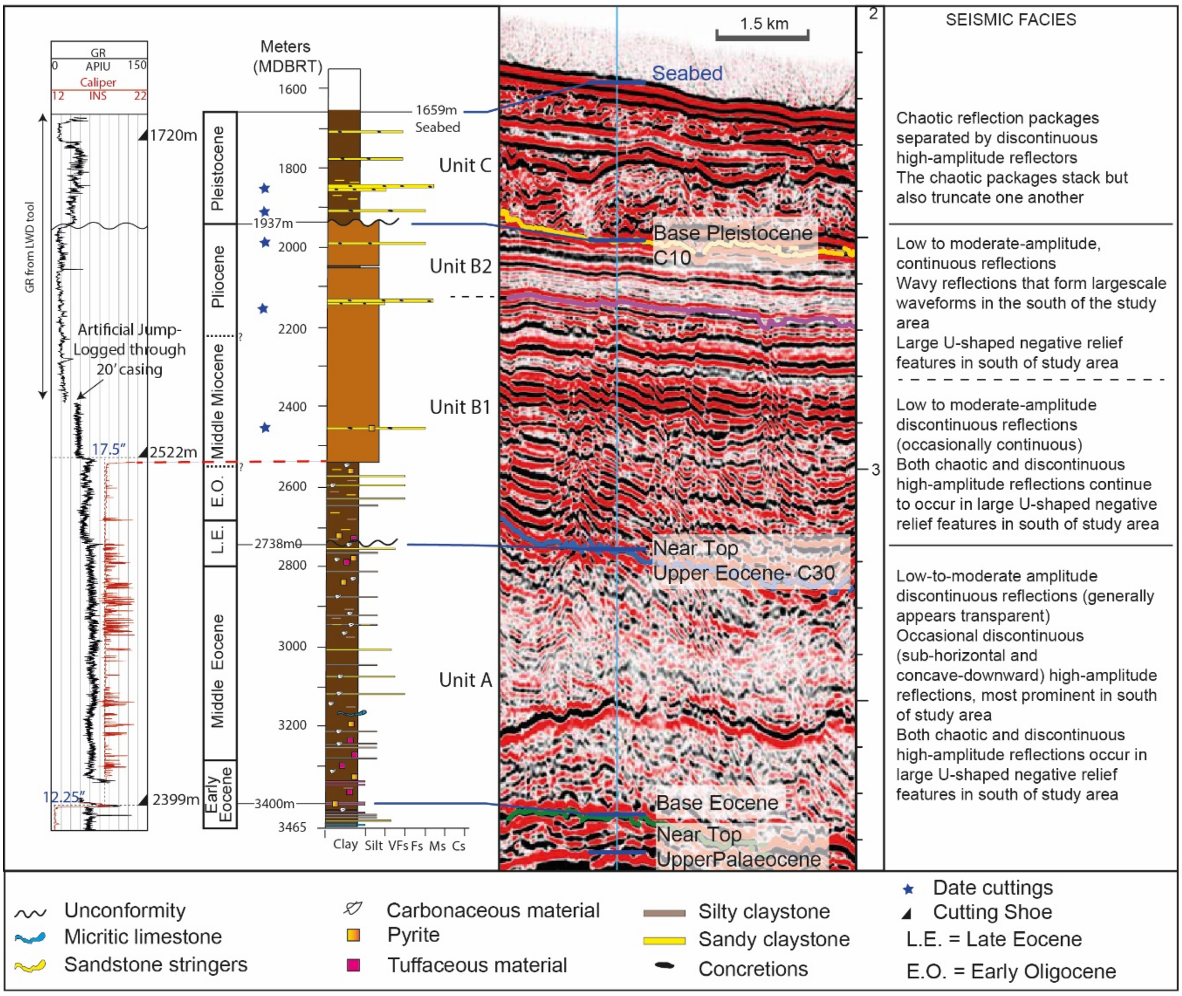

837

838

Figure 3

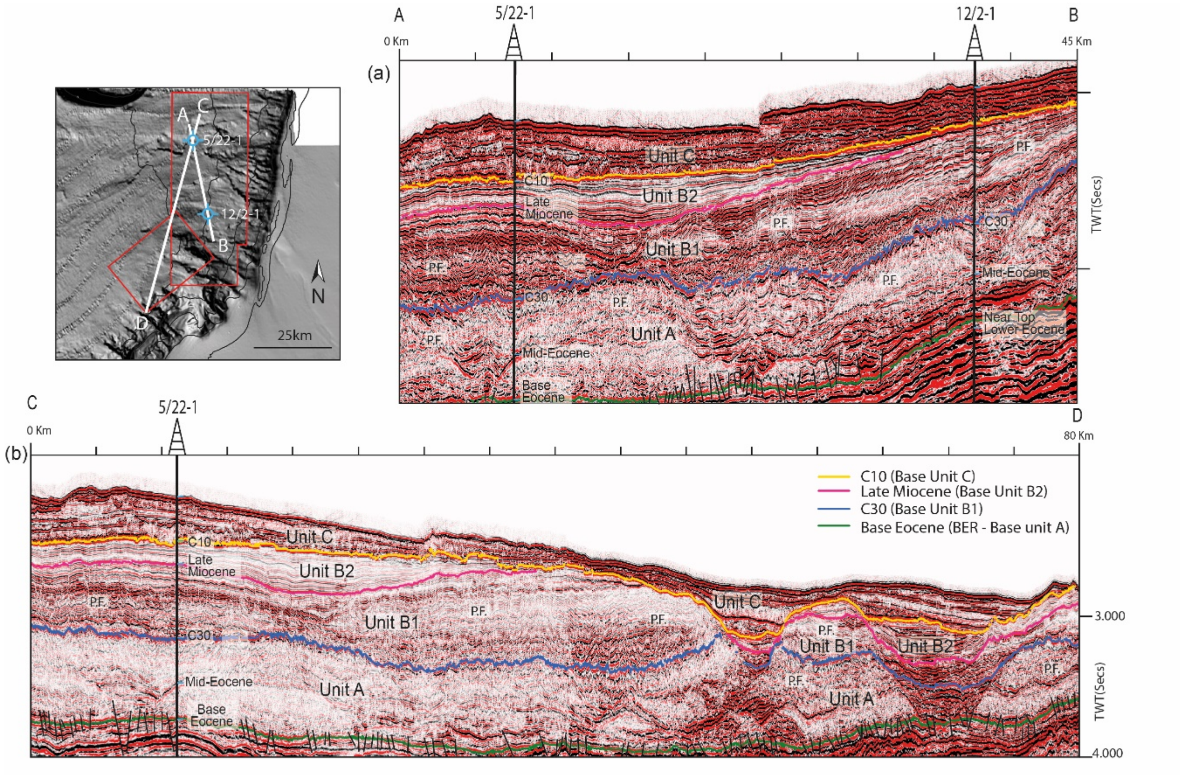

Figure 4

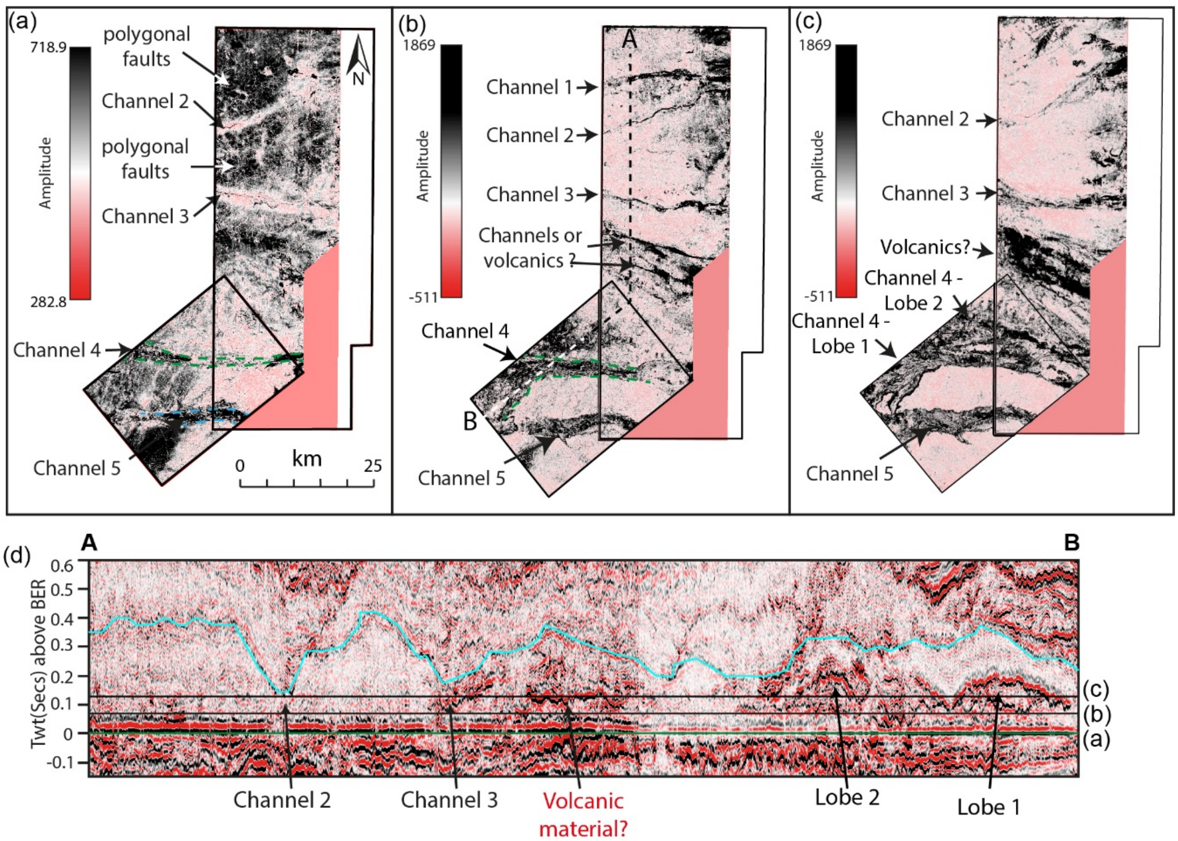

Figure 5

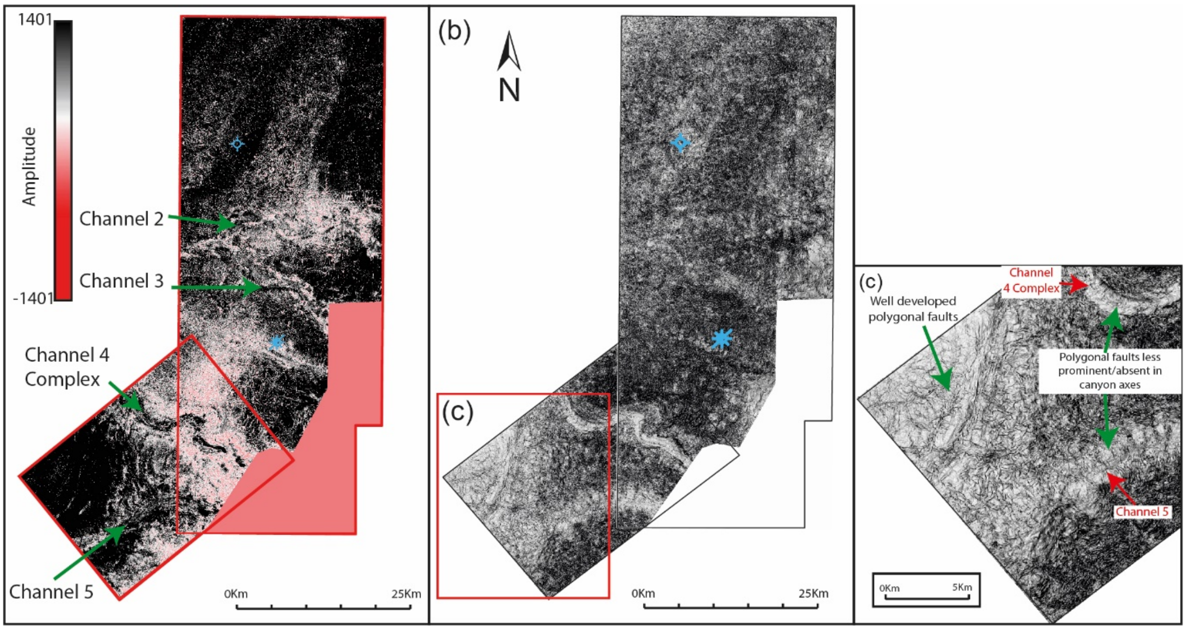

Figure 6

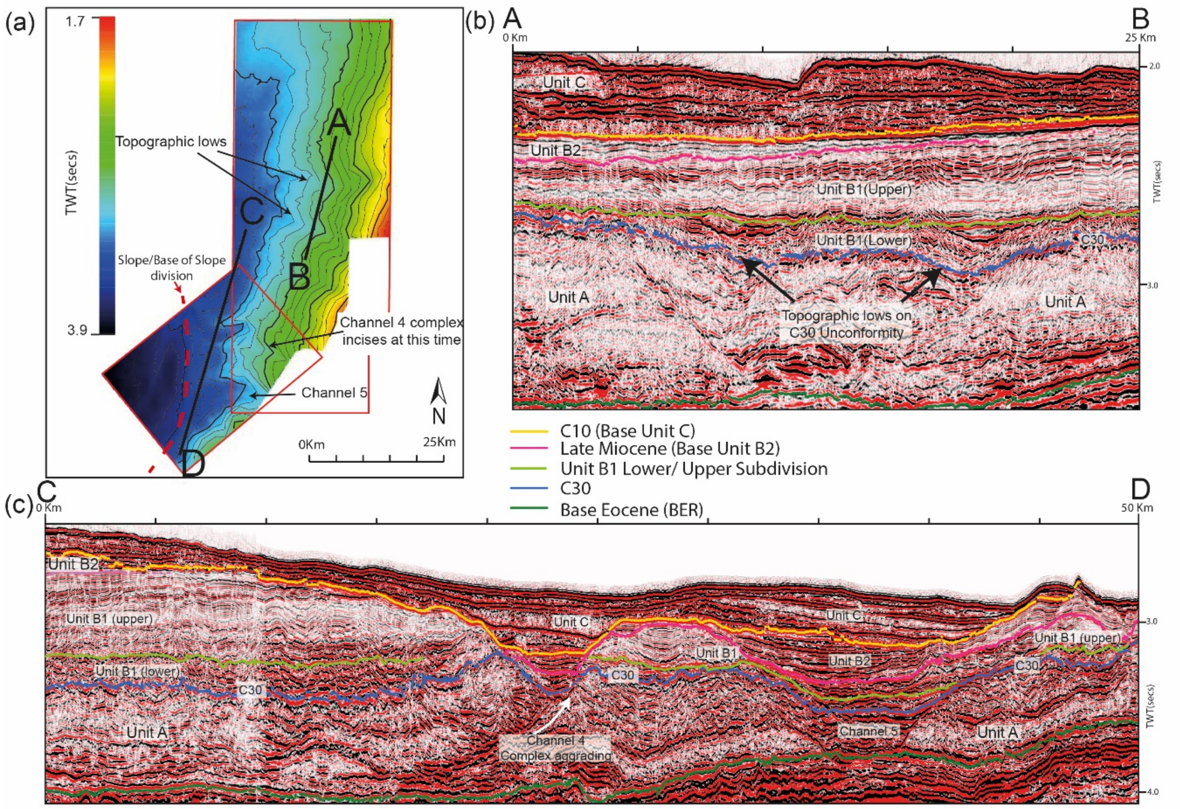

Figure 7

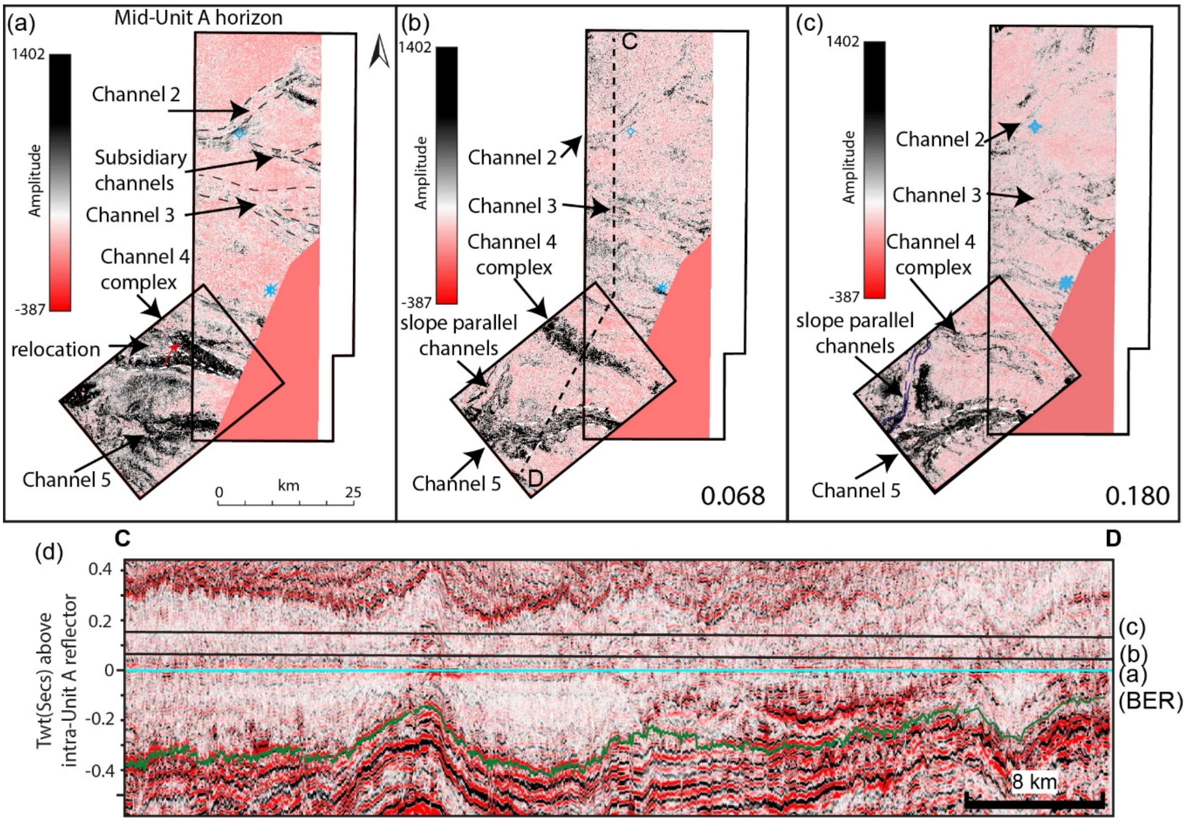

Figure 8

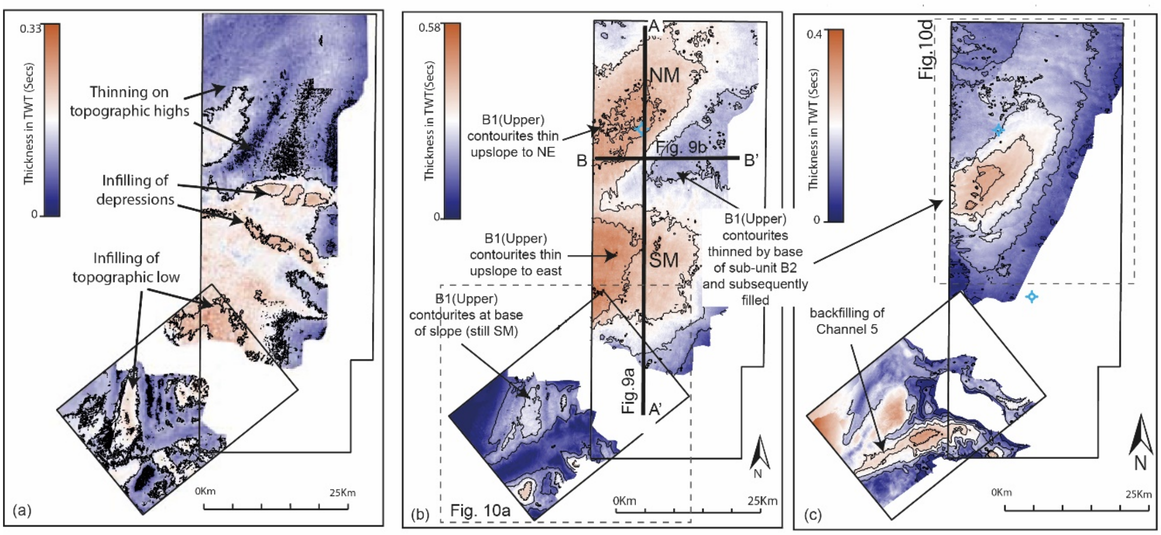

Figure 9

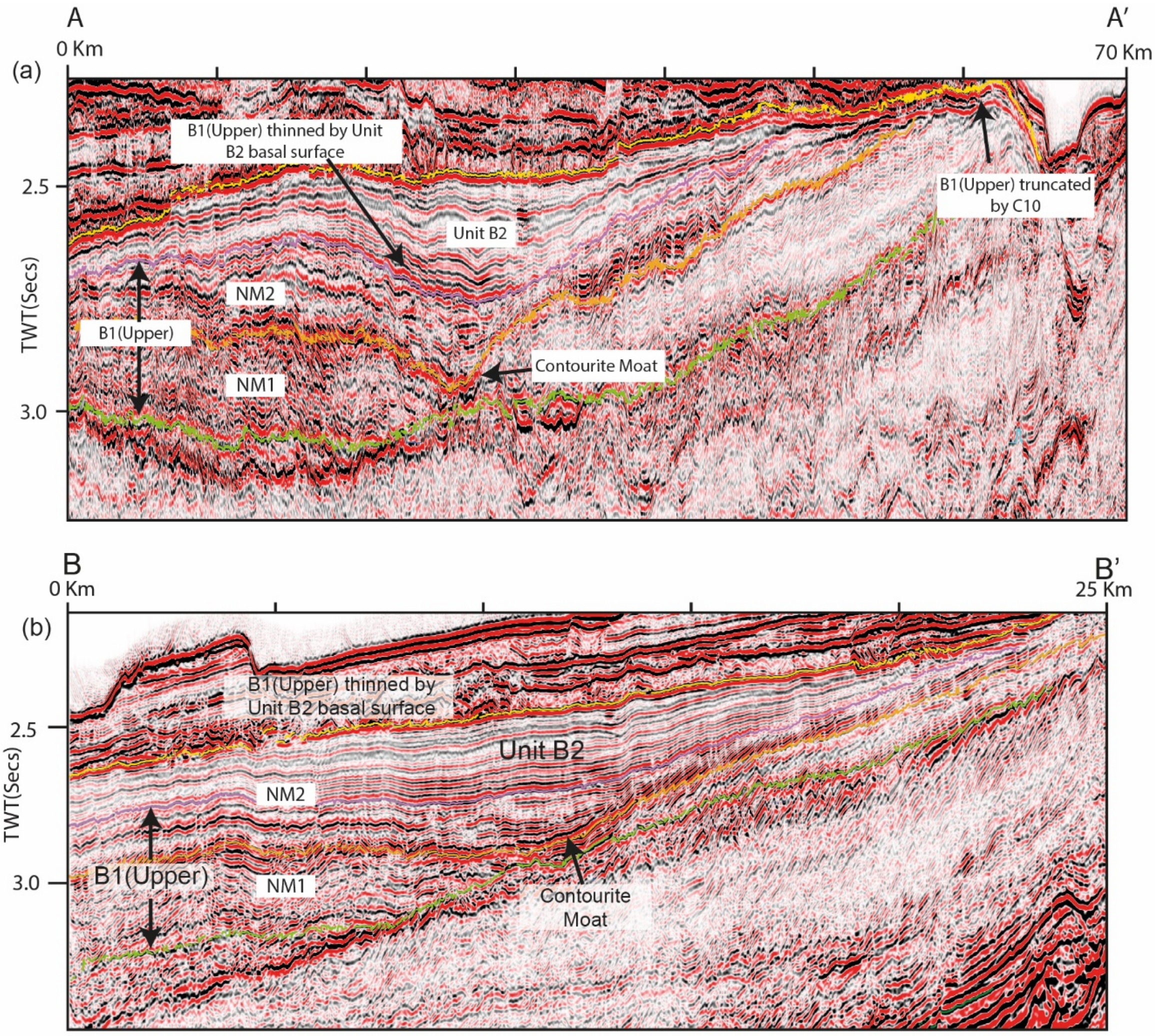
A
A′
0 Km
70 Km
(a)
B1(Upper) thinned by Unit B2 basal surface
B1(Upper) truncated by C10
Unit B2
NM2
B1(Upper)
NM1
Contourite Moat
TWT(Secs)
2.5
3.0
B
B'
0 Km
25 Km
(b)
B1(Upper) thinned by Unit B2 basal surface
Unit B2
NM2
B1(Upper)
NM1
Contourite Moat
TWT(Secs)
2.5
3.0

Figure 10

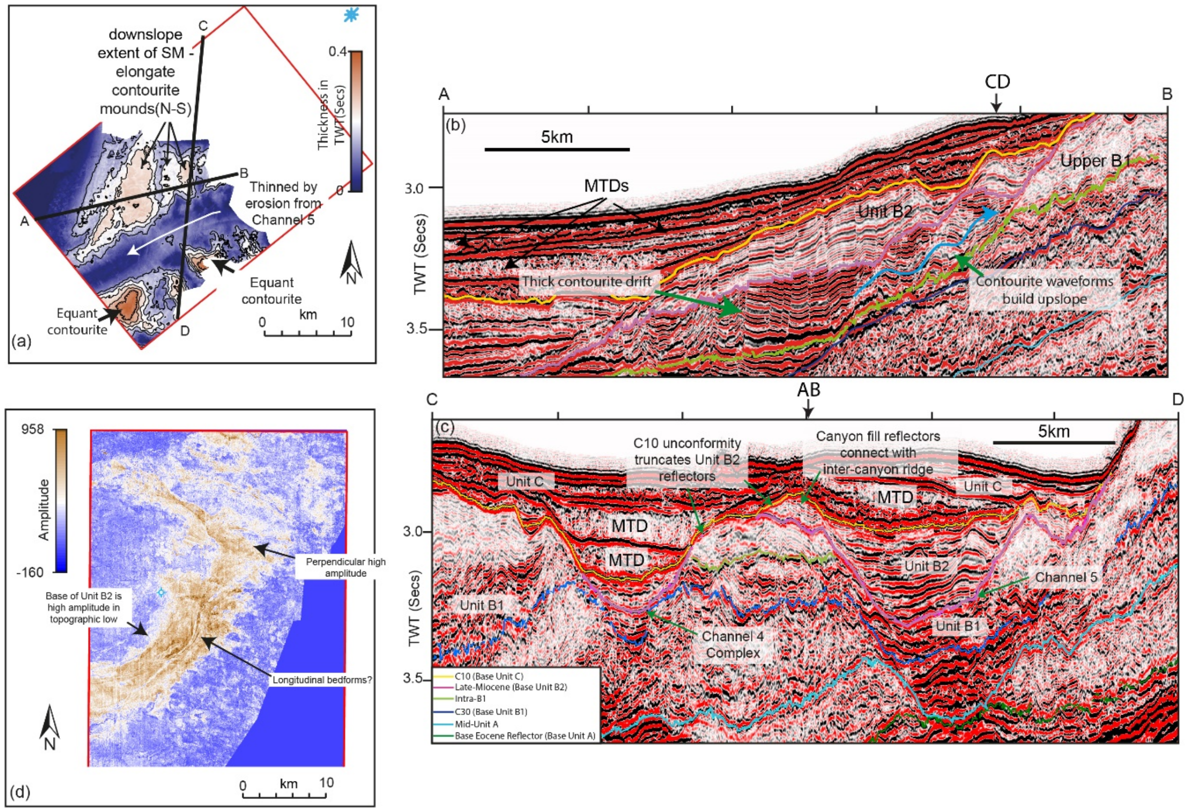
downslope extent of SM - elongate contourite mounds(N-S)
Thickness in TWT(Secs)
0.4
0
Thinned by erosion from Channel 5
Equant contourite
Equant contourite
km
0
10
(a)
A
B
C
D
N
A
CD
B
(b)
5km
MTDs
Unit B2
Upper B1
Thick contourite drift
Contourite waveforms build upslope
TWT (Secs)
3.0
3.5
C
AB
D
(c)
5km
C10 unconformity truncates Unit B2 reflectors
Canyon fill reflectors connect with inter-canyon ridge
Unit C
MTD
MTD
MTD
Unit C
Unit B2
Channel 5
Unit B1
Channel 4 Complex
Unit B1
C10 (Base Unit C)
Late-Miocene (Base Unit B2)
Intra-B1
C30 (Base Unit B1)
Mid-Unit A
Base Eocene Reflector (Base Unit A)
958
Amplitude
-160
Perpendicular high amplitude
Base of Unit B2 is high amplitude in topographic low
Longitudinal bedforms?
N
0
km
10
(d)

Figure 11

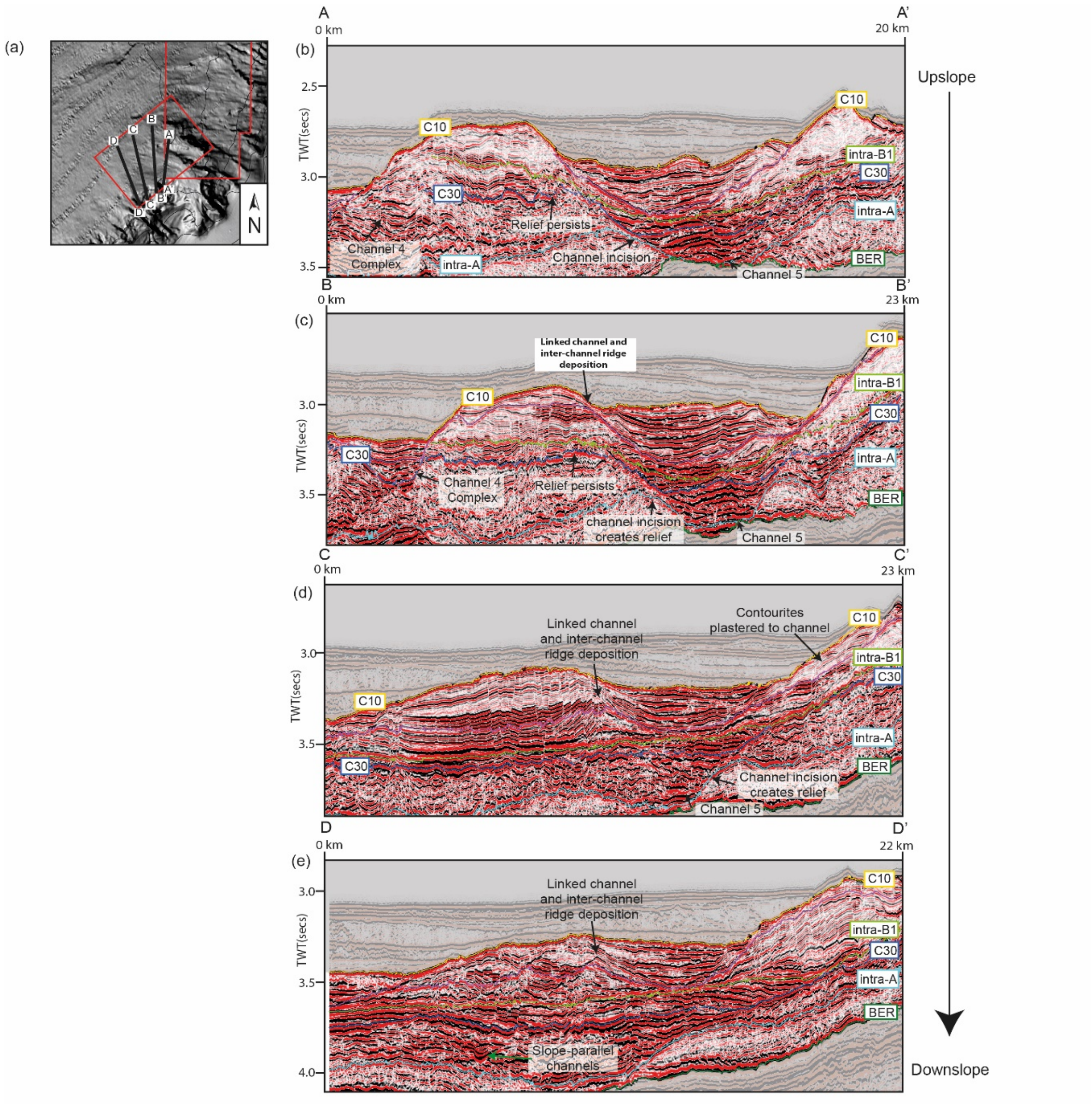
(a)
D
C
B
A
N
A
A'
0 km
20 km
(b)
TWT(secs)
2.5
3.0
3.5
C10
C10
intra-B1
C30
C30
intra-A
intra-A
BER
Relief persists
Channel 4 Complex
Channel incision
Channel 5
B
B'
0 km
23 km
(c)
Linked channel and inter-channel ridge deposition
C10
C10
intra-B1
C30
C30
intra-A
BER
Channel 4 Complex
Relief persists
channel incision creates relief
Channel 5
C
C'
0 km
23 km
(d)
Linked channel and inter-channel ridge deposition
Contourites plastered to channel
C10
C10
intra-B1
C30
C30
intra-A
BER
Channel incision creates relief
Channel 5
D
D'
0 km
22 km
(e)
4.0
Linked channel and inter-channel ridge deposition
C10
intra-B1
C30
intra-A
BER
Slope-parallel channels
Upslope
Downslope

863 Figure 12

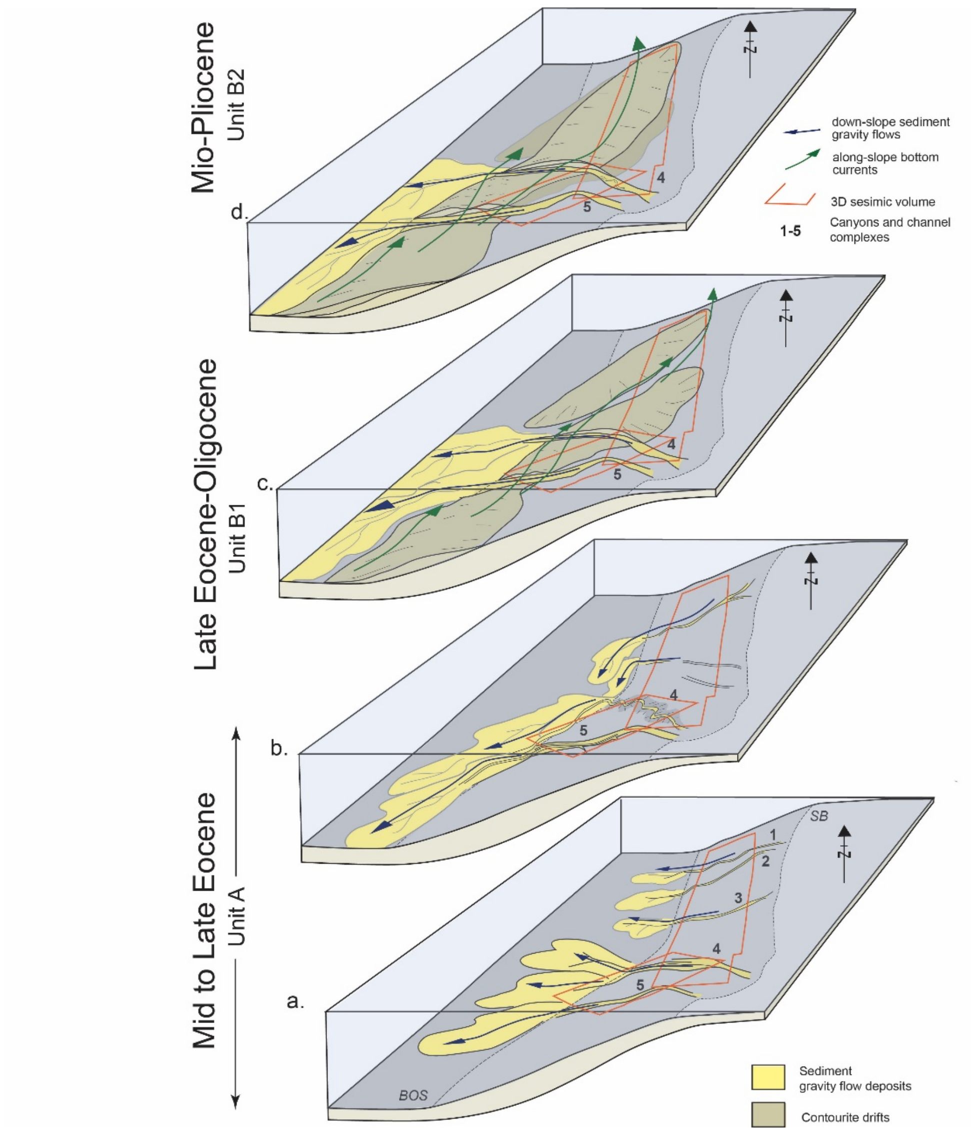

864

865

866 Figure 13

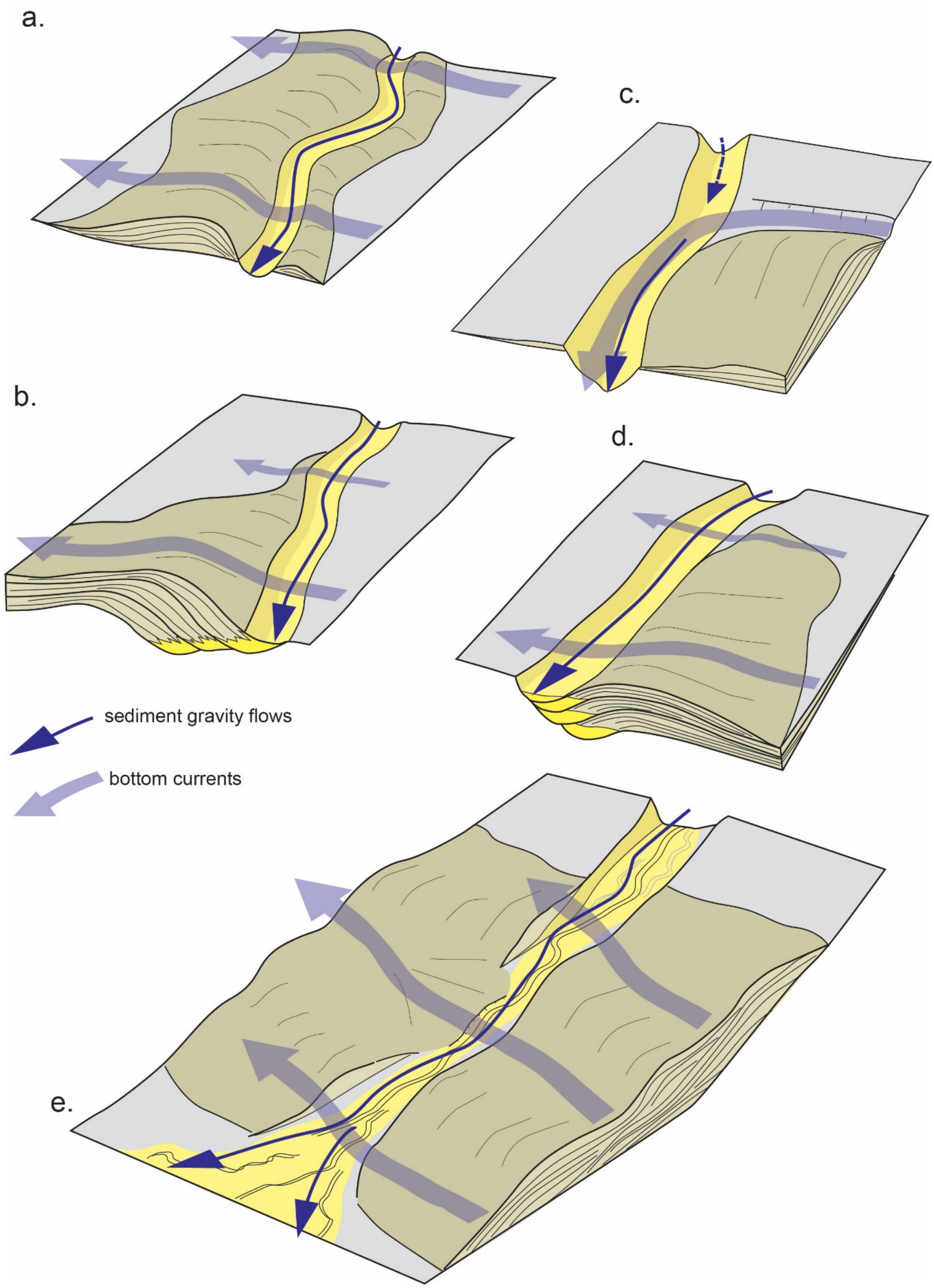

867